

High Order Difference Approximations for the Linearized Euler Equations

Stefan Johansson

Abstract

The computers of today make it possible to do direct simulation of aeroacoustics, which is very computationally demanding since a very high resolution is needed.

In the present thesis we study issues of relevance for aeroacoustic simulations. Paper A considers standard high order difference methods. We study two different ways of applying boundary conditions in a stable way. Numerical experiments are done for the 1D linearized Euler equations.

In paper B we develop strictly stable difference methods which give smaller dispersion errors than standard central difference methods. The new methods are applied to the 1D wave equation.

Finally in Paper C we apply the new difference methods to aeroacoustic simulations based on the 2D linearized Euler equations.

Taken together, the methods presented here are strictly stable by construction. They lead to better approximation of the wave number, which in turn results in a smaller L_2 -error than obtained by previous methods found in the literature. The results are valid when the problem is not fully resolved, which usually is the case for large scale applications.

Acknowledgments

First, I want to thank my supervisors Bernhard Müller and Mickael Tuné for all your support, and thoroughness in reviewing my work.

Finally, I wish to thank all the people at TDB for creating a good atmosphere, and supporting many interesting discussions.

List of Appended Papers

This thesis is a summary of the following papers. References to the papers are made using the capital letter associated with each paper.

Paper A Stefan Johansson. Numerical Solution of the Linearized Euler Equations Using High Order Finite Difference Operators with the Summation by Parts Property. Report 2002-034, Department of Information Technology, Uppsala University, Uppsala, 2002 (revised version, March 2003).

Paper B Stefan Johansson. High Order Finite Difference Operators with the Summation by Parts Property Based on DRP Schemes. Report 2004-036, Department of Information Technology, Uppsala University, Uppsala, 2004 Submitted to *BIT*.

Paper C Stefan Johansson. High Order Summation by Parts Operator Based on a DRP Scheme Applied to 2D Aeroacoustics. Report 2004-050, Department of Information Technology, Uppsala University, Uppsala, 2004.

Some numerical experiments from Paper A were presented by the author at the 10th International Congress on Sound and Vibration (2003) [7], together with work done by Bernhard Müller. Preliminary experiments using the new method from Paper B were included in joint papers with Bernhard Müller presented by Müller at EUROMECH Colloquium 449, Chamonix, France 2003 [6] and in Proceedings of 4th EC-COMAS Congress 2004, Jyväskylä, Finland [8]. The paper presented at EUROMECH will appear in Comptes Rendus Mecanique (2004/2005).

Contents

Summary

Paper A

Paper B

Paper C

1 Introduction

The development of methods for approximate solution of partial differential equations accelerated after the second world war due to the rapid development of computers that made it possible to solve non trivial problems. Partial differential equations are used by scientists to model wave propagation, heat transfer, fluid flow around rigid objects and many other applications.

Numerical analysis for partial differential equations, the subject of this thesis, is the art of approximating a partial differential equation, and thereafter solving the resulting algebraic problem. There are several alternative approaches to do the approximation. We have chosen the finite difference method, i.e., the variables are represented at grid points and derivatives are approximated using Taylor expansions. The reason for choosing finite difference methods is that they are relatively easy to implement, and in explicit form they are in most cases more efficient for wave propagation problems than for example the finite element method.

The computers of today make it possible to do direct simulation of aeroacoustics, which is very computationally demanding since a very high resolution is needed [13]. The application of aeroacoustics includes simulation of noise emitted from cars and airplanes. An example of such an application is the study by Johan Westerlund [15] where he studied rocket launch noise from a simplified model of the Ariane V rocket. A picture of acoustic pressure just before lift off is shown in Figure 1.

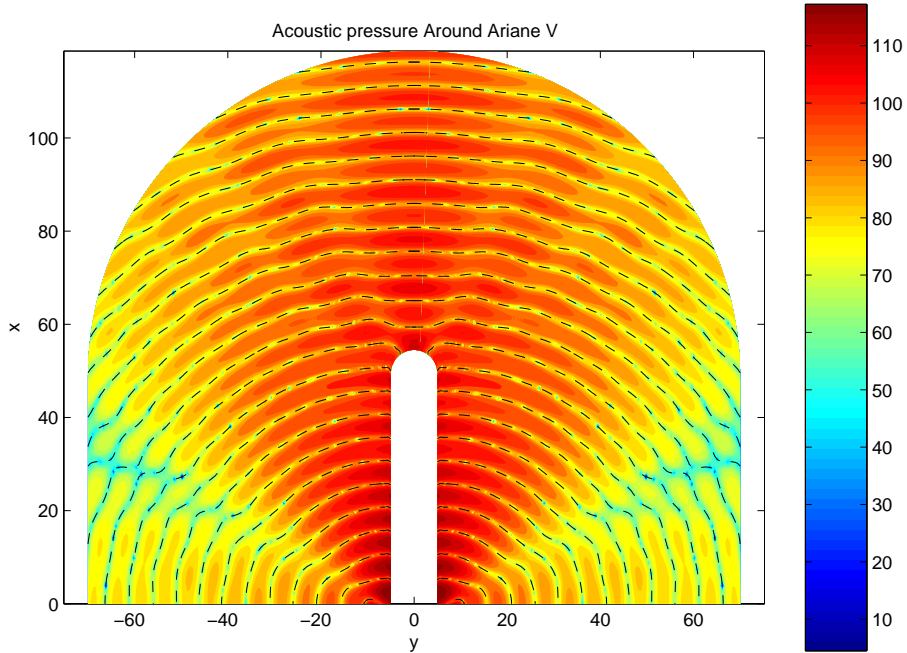


Figure 1: Solution for acoustic pressure measured in dB, when the frequency is 33 Hz.

In the present thesis we study issues of relevance for aeroacoustic simulations. Paper A considers standard high order difference methods. We

study two different ways to apply boundary conditions in a stable way. Numerical experiments are done for the 1D linearized Euler equations.

In paper B we develop strictly stable difference methods which give smaller dispersion errors than standard central difference methods. The new methods are applied to the 1D wave equation.

Finally in Paper C we apply the new difference methods to aeroacoustic simulations based on the 2D linearized Euler equations.

2 Overview of Stability Theory for Finite Difference Methods

Given a well-posed partial differential equation (PDE) there is no constructive way to write down the solution in closed form, and for many PDEs there are no known solutions in closed form. What can be done is to construct an approximation of the PDE that can be made arbitrary good that is "easy" to solve. One way of doing that is to approximate the derivatives with finite differences. Examples of finite differences for a grid function $u(t)_j = u(t, j * h)$, where h is the step size are

$$D_0 u_j = \frac{u_{j+1} - u_{j-1}}{2h} \quad D_- u_j = \frac{u_j - u_{j-1}}{h} \quad D_+ u_j = \frac{u_{j+1} - u_j}{h} \quad (1)$$

that can easily be shown to approach $\partial u / \partial x$ when $h \rightarrow 0$ by Taylor expansion.

The three important concepts for finite difference methods are consistency, stability and convergence. Consistency means that the approximation of the PDE converges to the PDE itself when letting the number of grid points go infinity, stability that the approximation in some sense is insensitive to perturbations of the initial data, boundary data and round off errors and convergence that the approximate solution approaches the exact solution when the number of grid points goes to infinity.

The connection between consistency, stability and convergence is given by the famous Lax-Richtmyer theorem that says that for a well-posed linear PDE a given consistent finite difference scheme is stable if and only if it is convergent.

Consistency of the method almost always follows from its construction, but the tricky part is to show stability, especially for initial boundary value problems. We start with the periodic case and let time be continuous, and look at the simplest hyperbolic PDE $u_t = u_x$, with initial condition $u(x, 0) = f$. Let us discretize $\partial/\partial x$ with D_0 . If the problem is periodic we can use the Fourier transform to investigate stability.

$$\frac{du_j}{dt} = \frac{u_{j+1} - u_{j-1}}{2h} \quad (2)$$

If we use Fourier transform formally on equation (2), the PDE transforms to an ordinary differential equation (ODE). For a wave number ω the ODE reads

$$\begin{aligned} \frac{de^{i\omega j h} \tilde{u}}{dt} &= \frac{1}{2h} \left(e^{i\omega(j+1)h} \tilde{u} - e^{i\omega(j-1)h} \tilde{u} \right) \Rightarrow \\ \frac{d\tilde{u}}{dt} &= \frac{1}{2h} \left(e^{i\omega h} e^{-i\omega h} \right) \tilde{u} \Rightarrow \frac{d\tilde{u}}{dt} = \frac{i}{h} \sin(\omega h) \tilde{u} \end{aligned} \quad (3)$$

It follows from Parseval's relation $\|\tilde{u}\| = \|u\|$ that the L_2 -norm of u is constant in time, because

$$\tilde{u}(\omega, t) = e^{\frac{i}{h} \sin(\omega h)t} \tilde{u}(\omega, 0) \Rightarrow \|\tilde{u}(\omega, t)\| = \|\tilde{u}(\omega, 0)\| \quad (4)$$

$$\underbrace{\Rightarrow}_{Parseval} \|u(\cdot, t)\| = \|u(\cdot, 0)\| \quad (5)$$

In general for the PDE $u_t = Pu$ the Fourier transform will yield $\tilde{u}(\omega, t) = e^{Qt} \tilde{u}(\omega, 0)$, where Q is the Fourier transform of P , and a sufficient condition for stability will be that the eigenvalues of Q have a non positive real part. For fully discrete approximations the condition is that the spectral radius of Q is less than or equal to $1 + \alpha k$, where α is a constant independent of x , h , and k and k is the time step. This method of investigating stability is also called von Neumann analysis.

The energy method can also be used. The idea is to show that the growth of the norm of u can be estimated independently of h .

The discrete scalar product is defined as $(u, v)_h = \sum_{j=0}^N u_j v_j h$, with the induced norm $\|u\|_h^2 = (u, u)_h$. For equation (2) the time derivative of $\|u\|$ is

$$\begin{aligned} \frac{d}{dt} \|u\| &= (u, u_t)_h + (u_t, u)_h = (u, D_0 u)_h + (D_0 u, u)_h = \\ &\quad - 2hu_0 u_{-1} + 2hu_N u_{N-1} = 0 \end{aligned} \quad (6)$$

That is the same result as we got using von Neumann analysis.

In general show that the approximation D of P is semi-bounded, i.e. $Re(v, Dv)_h \leq \alpha \|v\|_h^2 \forall v$ for some α independent of h , t and v . Then the energy estimate follows, since $d\|u\|/dt = (u_t, Du)_h + (Du, u_t)_h = 2Re(u, Du)_h$.

For initial boundary value problems the Fourier method cannot be used, the energy method on the other hand can be used. The calculation become more difficult, due to boundary terms that do not cancel as in the periodic case. They have to be estimated.

The most general technique for analyzing stability is the GKS method named after the authors of [5]: Bertil Gustafsson, Heinz-Otto Kreiss and Arne Sundström. The Laplace transform is applied in time and all but one space variable are Fourier transformed. That leads to an eigenvalue problem and the stability condition is that there are no eigenvalues with real part larger than zero.

For fully discrete initial boundary value problems both the energy method and the normal mode analysis also known as GKS method can be used to show stability, but the calculations in general become more difficult.

3 Paper A

In this paper high order difference schemes with the summation by parts (SBP) property were studied [11].

To use a SBP operator to discretize an initial boundary value problem (IVBP) the analytical boundary conditions must be imposed in a way that does not destroy the SBP property.

Currently there are two methods described in the literature, the projection method and the simultaneous approximation term (SAT) method.

The theory of the projection method can be found in [10] and is outlined here. Olsson's idea was that the boundary condition is fulfilled by projecting the discrete solution of the initial value problem to the vector space where the boundary condition is fulfilled. Using SBP operators he could give an energy estimate for the semi-discrete case.

Let the boundary condition be written in the form

$$\mathbf{L}^T v = g \quad (7)$$

were \mathbf{L} is a rectangular matrix, v the vector of unknowns and $g = g(t)$ a known function. Let \mathbf{H} be the diagonal positive definite matrix defining the discrete scalar product $(\cdot, \cdot)_h$. Then the matrix

$$\mathbf{P} = \mathbf{I} - \mathbf{H}^{-1} \mathbf{L} (\mathbf{L}^T \mathbf{H}^{-1} \mathbf{L})^{-1} \mathbf{L}^T \quad (8)$$

where \mathbf{I} is the identity matrix, defines a projection with the following properties

- $\mathbf{P}^2 = \mathbf{P}$
- $\mathbf{H}\mathbf{P} = \mathbf{P}^T \mathbf{H}$
- $v = \mathbf{P}v \Leftrightarrow \mathbf{L}^T v = 0$.

Given the linear advection equation

$$u_t + cu_x = 0 \quad (9)$$

were c is the advection speed. The projection method for the semi discrete problem becomes

$$v_t + \mathbf{P}c\mathbf{D}v = (\mathbf{I} - \mathbf{P})\tilde{g}_t \quad (10)$$

$$v(0) = f \quad (11)$$

where $\tilde{g} = [g, 0, \dots, 0]^T$ and f is the initial condition.

In the simultaneous approximation term (SAT) [2] method one does not impose the exact boundary conditions which might destroy the SBP property. Instead the boundary conditions are imposed as a penalty term at the same accuracy as the discretization.

Below is the SAT formulation for (9).

$$v_t + \mathbf{D}v = -\frac{\tau}{2h} H^{-1} e(L^T v - g(t)) \quad (12)$$

$$v(0) = f \quad (13)$$

where a bound on the parameter $\tau \geq 1$ is given by the energy method and $e = (1, 0, \dots, 0)^T$.

The two ways of imposing the boundary conditions were evaluated on the 1D isentropic linearized Euler equations. No noticeable differences were observed between the projection or SAT method, neither in accuracy

nor CPU time to solve the problem for the isentropic linearized Euler equations.

A comparison between initial data of different regularity was also performed, C^0 initial data and C^∞ initial data to be precise. As one may suspect the C^0 initial data lead to a solution with high frequency oscillations, but the oscillations did not affect the order of accuracy. However for non linear problems artificial dissipation has to be used to damp the oscillations which otherwise could grow exponentially [4].

4 Paper B

In aeroacoustics Dispersion Relation Preserving schemes (DRP) [14] have been given a lot of interest because the schemes have smaller dispersion error than standard finite difference schemes. The price you have to pay for that is to lower the formal accuracy of the method. Since the SBP method studied on Paper A is proven stable the question arises: Can we use DRP schemes instead of standard finite difference schemes in the SBP operator? The answer is yes, and the paper deals with the derivation of such difference operators.

Lets first explain the DRP schemes. If the formal accuracy of a finite difference method is lowered by two orders a free parameter is given that can be chosen such that the wave number is approximated better. The dimensionless wave number for the stencil $-\alpha_l \dots -\alpha_1 0 \alpha_1 \dots \alpha_l$ is $hk = \sum_{j=1}^l 2\alpha_j \sin(hk)$. The approximation of the wave number is good for small wave numbers and gets worse for larger wave numbers. The free parameter ϕ can be chosen such that DRP schemes gives a good approximation for larger wave numbers than standard finite difference schemes. For example one can minimize

$$E(\phi) = \int_{-\pi/2}^{\pi/2} |hk - h\tilde{k}(\phi)|^2 d(hk) \quad (14)$$

, where k and \tilde{k} are the exact and the approximate wave numbers, respectively. Figure 2 shows the approximate wave number for the 2nd and 6th order standard centered difference schemes and also a 4th order DRP scheme.

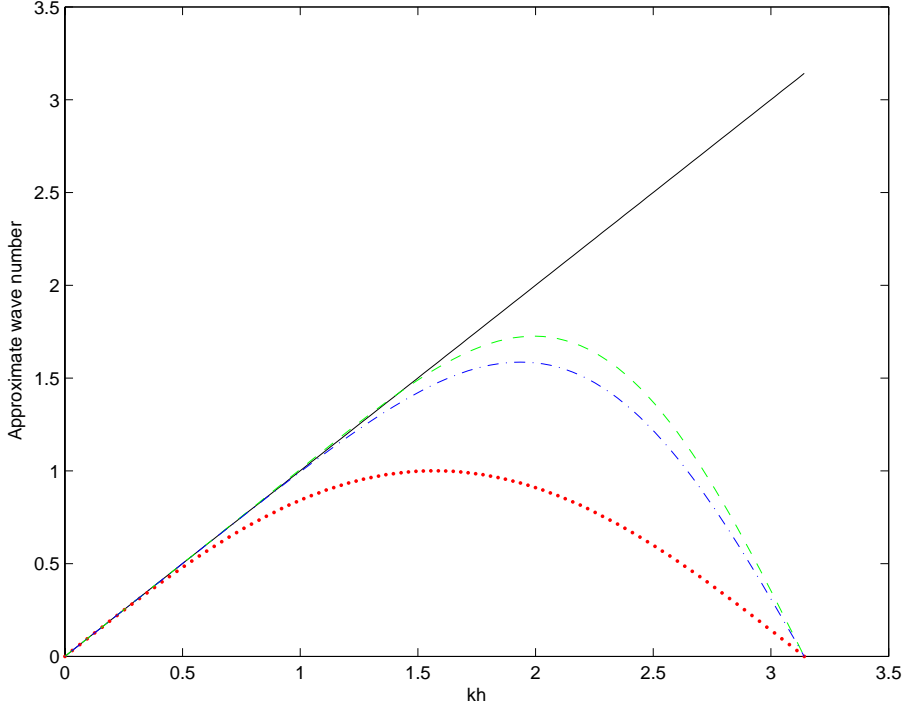


Figure 2: Approximate non-dimensional wave number vs exact for 2nd order standard centered difference method (SC2) (dotted), SC6 (dot-dashed), 4th order DRP scheme (dashed).

Given a DRP scheme of order 2τ with coefficients α_j , $j = 1 \dots \tau + 1$ a summation by parts operator Q which is accurate of order τ near the boundary and a diagonal norm matrix H with property that $h(HQ + (HQ)^T) = \text{diag}(-1, 0, \dots, 0, 1)$ will be derived.

For simplicity we approximate $\frac{d}{dx}$ for $x = [0, \infty)$ and let $h = 1$. The difference operator Q has to be modified for rows $1 \dots 2\tau$.

$$\left(\begin{array}{ccccccccc} q_{0,0} & q_{0,1} & \cdots & & q_{0,2\tau-1} & & & & \\ q_{1,0} & 0 & \ddots & & \vdots & q_{\tau-1,2\tau} & 0 & \cdots & \\ \vdots & \ddots & \ddots & & q_{2\tau-2,2\tau-1} & \vdots & \ddots & 0 & \cdots \\ q_{2\tau-1,0} & \cdots & q_{2\tau-1,2\tau-2} & & 0 & q_{2\tau-1,2\tau} & \cdots & q_{2\tau-1,3\tau} & 0 & \cdots \end{array} \right)$$

In order for HQ to be nearly antisymmetric and have the SBP property the following relations must hold

$$\begin{aligned} h_{0,0}q_{0,0} &= -1/2 \\ h_{i,i}q_{i,j} &= -h_{j,j}q_{j,i} \quad 0 \leq i < 2\tau - 1 \quad i < j \leq 2\tau - 1 \\ h_{i,i}q_{i,j} &= \alpha_{j-i} \quad \tau - 1 \leq i < 2\tau \quad 2\tau \leq j \leq \tau + i + 1 \end{aligned}$$

Requiring that polynomials of degree τ and lower are exactly differentiated by Q leads to $\tau + 1$ systems of equations. That together with the

conditions on HQ makes it possible to find closed expressions for Q and H .

The summation by parts operators for DRP schemes were tested for the 1D wave equation in first order form

$$u_t + \begin{pmatrix} 1 & 0 \\ 0 & -1 \end{pmatrix} u_x = 0, \quad u = \begin{pmatrix} u^I \\ u^{II} \end{pmatrix}, \quad 0 \leq x \leq 1, \quad t \geq 0,$$

With the initial data

$$u^I(x, 0) = \sin 2\pi x, \quad u^{II}(x, 0) = -\sin 2\pi x, \quad 0 \leq x \leq 1$$

and boundary conditions

$$u^I(0, t) = u^{II}(0, t), \quad u^{II}(1, t) = u^I(1, t), \quad t \geq 0,$$

The methods used in the numerical experiment were the second, third and fourth order DRPSBP methods, also denoted SBP- $\tau - 2\tau(2(\tau + 1))$. For the SBP-4-8(10) the free parameters were used to reduce the spectral radius of the method and therefore making it possible to use larger time steps. The parameters found reduced the spectral radius by about a factor of 10.

The global order of accuracy is given in Table 1 and is in agreement with theory, saying that the global accuracy is one order higher than the accuracy at the boundaries if the order in the interior is at least one order higher than the accuracy at the boundaries [3].

Table 1: Order of accuracy for u^I using SBP 2-4(6), SBP 3-6(8) and SBP 4-8(10) for the 1D test case at $t = 1.5$.

| # of grid points / | SBP 2-4(6) | SBP 3-6(8) | SBP 4-8(10) |
|--------------------|------------|------------|-------------|
| 101 | | | |
| 202 | 3.0137 | 3.9141 | 4.6758 |
| 401 | 3.0106 | 4.1361 | 4.6000 |
| 801 | 3.0083 | 4.3108 | 4.5678 |

The numerical experiments show that the DRPSBP method behaves according to theory in the 1D case. When taking into account that the 4th order Runge-Kutta was used in time, explaining the loss of accuracy for the SBP-4-8(10) cf. last column in Table 1. The next step is to evaluate the method on a 2D problem, which is done in the next paper, paper C.

5 Paper C

The 2D linearized Euler equations in conservative form [1] are used as a model of sound propagation. Denoting density ρ , velocity in x -direction u , in y -direction v , specific total energy E , specific total enthalphy H and pressure p . The equations are formulated in the variables ρ' , $(\rho u)'$, $(\rho v)'$ and $(\rho E)'$ that are perturbations of a reference state ρ_0 , $\rho_0 u_0$, $\rho_0 v_0$, $\rho_0 E_0$.

$$\begin{aligned} \frac{\partial}{\partial t} \begin{pmatrix} \rho' \\ (\rho u)' \\ (\rho v)' \\ (\rho E)' \end{pmatrix} + \frac{\partial}{\partial x} \begin{pmatrix} (\rho u)' \\ \rho_0 u_0 u' + (\rho u)' u_0 + p' \\ \rho_0 v_0 u' + (\rho v)' u_0 \\ \rho_0 H_0 u' + (\rho H)' u_0 \end{pmatrix} + \\ \frac{\partial}{\partial y} \begin{pmatrix} (\rho v)' \\ \rho_0 u_0 v' + (\rho u)' v_0 \\ \rho_0 v_0 v' + (\rho v)' v_0 + p' \\ \rho_0 H_0 v' + (\rho H)' v_0 \end{pmatrix} = 0 \quad (15) \end{aligned}$$

The acoustic quantities are defined by $\rho' = \rho - \rho_0$, $(\rho u)' = \rho u - \rho_0 u_0$, $(\rho v)' = \rho v - \rho_0 v_0$ and $(\rho E)' = \rho E - \rho_0 E_0$. With $(\rho H)' = (\rho E)' + p'$.

The variables u' , v' and p' can be calculated using

$$\mathbf{u}' = \frac{(\rho \mathbf{u})' - \rho' \mathbf{u}_0}{\rho_0} \quad (16)$$

$$p' = (\gamma - 1) \left((\rho E)' - \frac{1}{2} (2(\rho \mathbf{u})' \cdot \mathbf{u}_0 - \rho' \mathbf{u}_0 \cdot \mathbf{u}_0) \right) \quad (17)$$

with $\mathbf{u} = (u, v)^T$.

The high order SBP operator based on the Tam and Webb DRP scheme was implemented in a FORTRAN program [9] and tested for an aeroacoustic test problem from [12]. In the domain $[-100, 100] \times [-100, 100]$ the mean velocities were chosen as $u_0 = 0.5$, $v_0 = 0$. The initial conditions

$$p'(x, y, 0) = e^{-\log(2) \frac{x^2+y^2}{9}} \quad (18)$$

$$\rho'(x, y, 0) = e^{-\log(2) \frac{x^2+y^2}{9}} + 0.1e^{-\log(2) \frac{(x-67)^2+y^2}{25}} \quad (19)$$

$$u'(x, y, 0) = 0.04ye^{-\log(2) \frac{(x-67)^2+y^2}{25}} \quad (20)$$

$$v'(x, y, 0) = -0.04(x-67)e^{-\log(2) \frac{(x-67)^2+y^2}{25}} \quad (21)$$

result in an acoustic pulse first located at the center and propagating with the speed of sound in all directions transported by the mean velocity and entropy and vorticity waves propagating with the mean velocity originating near the right boundary.

The results were compared with those obtained with a third order SBP operator SBP-3-6 based on a sixth order standard central finite difference stencil.

The 2D linearized Euler equations were solved using those SBP operators to discretize x and y derivatives and using the standard fourth order Runge-Kutta method to discretize the time derivative.

The numerical results for the 2D linearized Euler equations show that the better approximation of the wave number for the DRP based SBP operator of fourth order (second order near the boundary) results in a smaller L_2 -error than for a SBP operator based on standard sixth order (third order near the boundary) stencil. The results are valid when the problem is not fully resolved, which usually is the case for large scale applications.

Application of a sixth order filter affects the good wave approximation of the DRPSPB operator. That problem can be solved by using a filter or artificial dissipation that apply less dissipation for wave numbers $hk < \pi/2$ than the present filter.

The development and implementation of accurate non reflecting boundary conditions is future work.

References

- [1] M. Billson, L.-E. Eriksson, and L. Davidson. Acoustic Source Terms for the Linear Euler Equations on Conservative Form. In *8th AIAA/CAES Aeroacoustics Conference*, Breckenridge, Colorado, (2002). AIAA Paper 2002-2582.
- [2] M.H. Carpenter, D. Gottlieb, and S. Abarbanel. Time-Stable Boundary Conditions for Finite-Difference Schemes Solving Hyperbolic Systems: Methodology and Application to High-Order Compact Schemes. *J. Comp. Phys.*, 111:220–236, (1994).
- [3] B. Gustafsson. The Convergence Rate for Difference Approximations to Mixed Initial Boundary Value Problems. *Math. Comp.*, 29(130):396–406, (1975).
- [4] B. Gustafsson, H.-O. Kreiss, and J. Oliger. *Time Dependent Problems and Difference Methods*. John Wiley & Sons, New York, (1995).
- [5] B. Gustafsson, H.-O. Kreiss, and A. Sundström. Stability Theory of Difference Approximations for Mixed Initial Boundary Value Problems. II. *Math. Comp.*, 26(119):649–686, (1972).
- [6] B. Müller and S. Johansson. Strictly Stable High Order Difference Approximations for Computational Aeroacoustics. In *Computational Aeroacoustics: From Acoustic Sources Modeling to Far-Field Radiated Noise Prediction*, EUROMECH Colloquium 449, (2003).
- [7] B. Müller and S. Johansson. Strictly Stable High Order Difference Approximations for the Euler Equations. In *Proceedings of the Tenth International Congress on Sound and Vibration*, (2003).
- [8] B. Müller and S. Johansson. Strictly Stable High Order Difference Approximations for Low Mach Number Aeroacoustics. In P. Neittaanmäki, T. Rossi, K. Majava, and O. Pironneau, editors, *ECCOMAS 2004*, (2004).
- [9] C. L. Müller. *High order accurate numerical solution of the linearized Euler equations for sound propagation in the atmosphere*. Master's thesis, Uppsala University, Department of Scientific Computing, (2004).
- [10] P. Olsson. Summation by Parts, Projections, and Stability. I. *Math. Comp.*, 64:1035–1065, (1995).
- [11] B. Strand. Summation by Parts for Finite Difference Approximations for d/dx . *J. Comp. Phys.*, 110:47–67, (1994).
- [12] C.K.W. Tam. Benchmark Problems and Solutions. In J.C. Hardin, J.R. Ristorcelli, and C.K.W. Tam, editors, *ICASE/LaRC Workshop on Benchmark Problems in Computational Aeroacoustics (CAA)*, (1995). NASA CP 3300.
- [13] C.K.W Tam. Computational aeroacoustics: Issues and methods. *AIAA J.*, 33:1788–1796, (1995).

- [14] C.K.W Tam and J. C. Webb. Dispersion-Relation-Preserving Finite Difference Schemes for Computational Acoustics. *J. Comp. Phys.*, 107:262–281, (1993).
- [15] J. Westerlund. *High order Simulation of Rocket Launch Noise*. Master’s thesis, Uppsala University, Department of Scientific Computing, (2002).

Paper A

Paper B

Paper C

NUMERICAL SOLUTION OF THE
LINEARIZED EULER EQUATIONS USING
HIGH ORDER FINITE DIFFERENCE
OPERATORS WITH THE SUMMATION BY
PARTS PROPERTY

Stefan Johansson

Department of Information Technology
Scientific Computing
Uppsala University
P.O. Box 337
SE 75105, Uppsala
Sweden

Abstract

We have used high order finite difference methods with the summation by parts property (SBP) on the 1D linearized Euler equations. The boundary conditions are imposed with both the projection method and the simultaneous approximation term method (SAT) for comparison. The formal fourth order of accuracy of the high order SBP operator was verified with both the projection method and the SAT method. Some relatively large errors were observed at the artificial boundaries and further investigations are needed to improve the non-reflecting boundary conditions.

Key words: linearized Euler equations, computational aeroacoustics, high order difference method, summation by parts, non-reflecting boundary conditions

1 Introduction

Most natural phenomena of interest are governed by partial differential equations (PDEs), yet no general technique is known to find the exact solution to a given well-posed PDE. Therefore numerical methods have been used even long before the birth of digital computers, see for example the work by L. F. Richardson [9].

PDEs governing acoustics often require high order methods to reach accuracy requirements: low dissipation and dispersion errors, cf. Tam [11].

To exemplify there are large scale disparities between the eddy scale l and the acoustic wavelength $\lambda \sim lM^{-1}$, where M is the Mach number. There are also large energy density disparities between the hydrodynamic near field and the acoustic far field cf. [4].

A technique that can be used to avoid resolving the different scales was proposed by Lighthill [7] in the 1950's where one first solves the flow field and uses that solution as a source term to the wave equation to get the acoustic field.

The linearized Euler equations have received interest since they can be used to model refractive effects and reflections at solid boundaries cf. M. Billson et al. [1]. Direct simulation of these phenomena has come into reach for our computers only in recent years.

In the numerical experiments I have studied isentropic and non isentropic sound propagation, governed by the linearized Euler equations in one space dimension. Discretization was done with a finite difference method, more precisely with a high order summation by parts operator (SBP) [6][10]. The boundary conditions were imposed with the simultaneous approximation term method (SAT) introduced by Carpenter et al. [2] and in some cases by the projection method described by Olsson [8]. The classical four step Runge-Kutta method was used for time marching.

The most important advantage of the summation by parts operators is that they lead to strictly stable high order finite difference methods.

The goal of this investigation was to check the accuracy of the summation by parts operator for the linearized Euler equations and to compare the simultaneous approximation term method and the projection method both used to impose boundary conditions.

2 The governing equations

The 1D nonlinear Euler equations read

$$\mathbf{u}_t + \mathbf{A}\mathbf{u}_x = 0 \quad (1)$$

where $\mathbf{u} = (\rho, u, p)^T$ and

$$\mathbf{A} = \begin{pmatrix} u & \rho & 0 \\ 0 & u & 1/\rho \\ 0 & \gamma p & u \end{pmatrix} \quad (2)$$

where u is the velocity, p is the pressure and ρ is the density. Time is denoted by t , x is the space coordinate and γ is the ratio of specific heats, here $\gamma = 1.4$ for air. We then linearize around the mean values (R, U, P) . We replace u by $U + \epsilon u'$ and analogous for p and ρ , and neglect high order terms of $\mathcal{O}(\epsilon^2)$ and get

$$\mathbf{u}'_t + \mathbf{B}\mathbf{u}'_x = 0 \quad (3)$$

where $\mathbf{u}' = (\rho', u', p')^T$ and

$$\mathbf{B} = \begin{pmatrix} U & R & 0 \\ 0 & U & 1/R \\ 0 & \gamma P & U \end{pmatrix} \quad (4)$$

The eigenvalues of \mathbf{B} are $U - a$, U and $U + a$, the corresponding eigenvectors are the columns in the matrix

$$\mathbf{R} = \begin{pmatrix} R/a & 1 & R/a \\ -1 & 0 & 1 \\ Ra & 0 & Ra \end{pmatrix} \quad (5)$$

with inverse

$$\mathbf{R}^{-1} = \begin{pmatrix} 0 & -1/2 & 1/(2Ra) \\ 1 & 0 & -1/a^2 \\ 0 & 1/2 & 1/(2Ra) \end{pmatrix} \quad (6)$$

where $a = \gamma P/R$ is the speed of sound. The linearized Euler equations are often used to model sound propagation.

To simplify things we can assume that the change in entropy is zero, the so called isentropic case. Then

$$\frac{p}{p_\infty} = \left(\frac{\rho}{\rho_\infty} \right)^\gamma = \left(\frac{T}{T_\infty} \right)^{\frac{\gamma}{\gamma-1}} \quad (7)$$

where the subscript ∞ denotes a reference state and T is temperature.

The 1D linearized Euler equations for the isentropic case read

$$\mathbf{u}'_t + \mathbf{C}\mathbf{u}'_x = 0 \quad (8)$$

where

$$\mathbf{C} = \begin{pmatrix} U & a \\ a & U \end{pmatrix} \quad (9)$$

and $\mathbf{u}' = (u', \rho')^T$. U , a , u' and ρ' are the mean flow velocity, mean speed of sound, velocity and density perturbations, respectively. In the following, the prime ' to indicate perturbation variables will be omitted i.e. from here on, we use the notation $u = u'$ and $\rho = \rho'$, if not stated otherwise. The eigenvalues of \mathbf{A} are $U - a$ and $U + a$, and the corresponding eigenvectors are the columns in

$$\mathbf{R} = \frac{1}{\sqrt{2}} \begin{pmatrix} 1 & 1 \\ 1 & -1 \end{pmatrix}. \quad (10)$$

Define $\mathbf{w} = \mathbf{R}^{-1}\mathbf{u}'$ then we can multiply the above systems (3) and (8) from the left by \mathbf{R}^{-1} to get

$$\mathbf{w}_t + \mathbf{\Lambda w}_x = 0 \quad (11)$$

where $\mathbf{\Lambda}$ is a diagonal matrix containing the eigenvalues λ_i of \mathbf{B} and \mathbf{C} , respectively.

The reason for transforming the system is to be able to use the SAT method described in section 5 for implementing non-reflecting boundary conditions and derive exact solutions.

3 Summation by parts operators

When doing numerical calculations we must establish an upper bound on the growth of the solution. In the continuous case the energy method is often used, for example, with the usual L^2 scalar product and norm

$$(u, v) = \int_a^b uv dx, \quad \|u\| = (u, u)^{1/2}. \quad (12)$$

We have for the simplest hyperbolic equation, sometimes called the Kreiss equation,

$$u_t = u_x \quad (13)$$

the following energy growth

$$\frac{1}{2} \frac{d\|u\|^2}{dt} = (u, u_t) = (u, u_x) = \frac{1}{2} [u^2]_a^b. \quad (14)$$

That is the energy growth in time is governed by the boundary values. In the last step, we used integration by parts

$$(u, v_x) = [uv]_a^b - (u_x, v) \quad (15)$$

In the discrete case we want to find an operator \mathbf{D} and a scalar product H that approximates the derivative d/dx and the integral \int_a^b with the same properties as the continuous case.

$$(u, \mathbf{D}v)_h = u_n v_n - u_0 v_0 - (\mathbf{D}u, v)_h \quad (16)$$

where

$$(u, v)_h = h u^T \mathbf{H} v, \text{ where } h \text{ is the step size.} \quad (17)$$

Since equation (16) is the discrete analogue of equation (15), it is called summation by parts property.

An example of such an operator D and scalar product H is

$$\mathbf{D} = \frac{1}{h} \begin{pmatrix} -1 & 1 & 0 & \dots & 0 \\ -0.5 & 0 & 0.5 & \ddots & \vdots \\ 0 & \ddots & \ddots & \ddots & 0 \\ \vdots & \ddots & -0.5 & 0 & 0.5 \\ 0 & \dots & 0 & -1 & 1 \end{pmatrix}, \mathbf{H} = \begin{pmatrix} 0.5 & 0 & \dots & & 0 \\ 0 & 1 & 0 & & \\ \vdots & \ddots & \ddots & \ddots & \vdots \\ & & 0 & 1 & 0 \\ 0 & & \dots & 0 & 0.5 \end{pmatrix}.$$

Operators of this kind were described by Kreiss and Scherer [6], and high order operators were later constructed by Strand [10]. High order operators \mathbf{D} have the following structure: in the interior a standard centered high order finite difference stencil is used and near the boundary when the standard stencil cannot be used, a small dense matrix is used instead. E.g. the boundary matrix giving third order is 6×9 . The stencil giving sixth order and that boundary matrix giving third order are given in the Appendix. For diagonal norms \mathbf{H} Strand [10] constructed matrices \mathbf{Q} giving order $s = 1, \dots, 4$ corresponding to stencils of order $2s$ in the interior.

4 Projection method

To apply high order operators of the SBP type to an initial boundary value problem (IVBP) the analytical boundary conditions must be satisfied in a certain way in order not to destroy the SBP property. Currently there are two popular methods, the projection method and the simultaneous approximation term (SAT) method. The latter method will be described in the next section. The theory of the projection method can be found in [8] and is outlined here. Olsson's idea was that the boundary condition was fulfilled by projecting the discrete solution to the initial value problem to the vector space where it is fulfilled. Using SBP operators he could give an energy estimate for the semi-discrete case.

Let the boundary condition be written in the form

$$\mathbf{L}^T v = g \tag{18}$$

where \mathbf{L} is a rectangular matrix, v the vector of unknowns and $g = g(t)$ a known function. Then the matrix

$$\mathbf{P} = \mathbf{I} - \mathbf{H}^{-1} \mathbf{L} (\mathbf{L}^T \mathbf{H}^{-1} \mathbf{L})^{-1} \mathbf{L}^T \tag{19}$$

where I is the identity matrix, defines a projection with the following properties

- $\mathbf{P}^2 = \mathbf{P}$
- $\mathbf{H}\mathbf{P} = \mathbf{P}^T\mathbf{H}$
- $v = \mathbf{P}v \Leftrightarrow \mathbf{L}^T v = 0$.

Given the linear advection equation

$$u_t + cu_x = 0 \tag{20}$$

were c is the advection speed. The projection method for the semi discrete problem becomes

$$v_t + \mathbf{P}c\mathbf{D}v = 0 \quad (21)$$

$$v(0) = f \quad (22)$$

where f is the initial condition. In general the right hand side in (21) involves time derivatives of g , but in our case it is zero because we implement non-reflecting boundary conditions.

Given two matrices $\mathbf{A}_{m,n}$ and $\mathbf{B}_{p,q}$. The Kronecker product \otimes is defined as

$$\mathbf{A} \otimes \mathbf{B} = \begin{pmatrix} a_{1,1}\mathbf{B} & \dots & a_{1,n}\mathbf{B} \\ \vdots & & \vdots \\ a_{m,1}\mathbf{B} & \dots & a_{m,n}\mathbf{B} \end{pmatrix}.$$

For systems the projection method can be expressed using the Kronecker product

$$v_t + (\mathbf{I} \otimes \mathbf{P})(\mathbf{I}_{N,N} \otimes \mathbf{C})(\mathbf{D} \otimes \mathbf{I})v = 0 \quad (23)$$

$$v(0) = f \quad (24)$$

were $\mathbf{I}_{N,N}$ is the identity matrix of dimension $N \times N$, \mathbf{C} is the diagonal matrix $diag[c, \dots, c]^T$ the dimension of the identity matrix \mathbf{I} is the same as the number of equations (in our case we have two equations) in the system, and the values in v and f are ordered vector wise, for example $v = [u_0, \rho_0, u_1, \rho_1, \dots, u_N, \rho_N]^T$.

5 Simultaneous approximation term

In the SAT method one does not impose the exact boundary conditions (b.c.) which might destroy the SBP property and can lead to time-instabilities i.e. the solution can suddenly blow up if you calculate long enough in time. Instead the boundary conditions are imposed as a penalty term at the same accuracy as the discretization. Below is the SAT formulation for (3) and is analogous for (8). We start with the semi-discrete form of (3).

$$\mathbf{v}_t + \mathbf{D} \otimes \mathbf{B} \mathbf{v} = 0 \quad (25)$$

and for systems the SAT method reads:

$$\mathbf{v}_t + (I_{N,N} \otimes \mathbf{B})(\mathbf{D} \otimes I)\mathbf{v} = SAT \quad (26)$$

were $I_{N,N}$ is the identity matrix of dimension $N \times N$, n is the number of equations in the system, the dimension of the identity matrix I is n , and the values in v are ordered vector wise, for example $\mathbf{v} = [u_0, \rho_0, u_1, \rho_1, \dots, u_N, \rho_N]^T$. where

$$SAT_j = \begin{cases} -h_{00}^{-1}\mathbf{R}(\Lambda^+\mathbf{R}^{-1}v_0 - \Phi_0(t))h^{-1}, & j=0, \\ 0, & 0 < j < N, \\ h_{NN}^{-1}\mathbf{R}(\Lambda^-\mathbf{R}^{-1}v_N - \Phi_N(t))h^{-1}, & j=N, \end{cases} \quad (27)$$

h_{00} and h_{NN} are the first and last elements of the norm matrix H and $\Lambda^\pm = \frac{1}{2}(\Lambda \pm |\Lambda|)$, with $|\Lambda| = diag(|\lambda_i|)$. Non-reflecting boundary conditions are implemented by $\Phi_0(t) = \Phi_N(t) = 0$

6 The classical Runge-Kutta method for ODE's

Using a summation by parts operator in the system

$$u_t + \mathbf{A}u_x = 0 \quad (28)$$

gives a large system of ODE's

$$v_t = \mathbf{P}v \quad (29)$$

where \mathbf{P} is a discrete approximation of $-\mathbf{A}\frac{d}{dx}$.

To solve this system we use the classical Runge-Kutta method [3], which is fourth order accurate.

$$v^{(1)} = v^n \quad (30)$$

$$v^{(2)} = v^n + \frac{1}{2}\Delta t \mathbf{P}v^{(1)} \quad (31)$$

$$v^{(3)} = v^n + \frac{1}{2}\Delta t \mathbf{P}v^{(2)} \quad (32)$$

$$v^{(4)} = v^n + \Delta t \mathbf{P}v^{(3)} \quad (33)$$

$$v^{n+1} = v^n + \Delta t \left(\frac{1}{6} \mathbf{P}v^{(1)} + \frac{1}{3} \mathbf{P}v^{(2)} + \frac{1}{3} \mathbf{P}v^{(3)} + \frac{1}{6} \mathbf{P}v^{(4)} \right). \quad (34)$$

7 Numerical experiments

The test cases are now described in more detail. The equations used are the linearized isentropic Euler equations (8) and the linearized Euler equations (3), with a sine pulse in the isentropic case and a Gaussian in the non-isentropic case.

7.1 Isentropic test case

The initial values given are

$$u'(x, 0) = \begin{cases} (\sin \frac{x-0.4}{0.2}\pi)^4 & \text{if } 0.4 \leq x \leq 0.6 \\ 0 & \text{otherwise} \end{cases}$$

The initial density perturbation ρ' is set to zero, and the Mach number $M = U/a$ is 0.5.

The solution to the acoustic velocity field and the acoustic density field there are two waves traveling in opposite directions and at different speeds ($U+a=1$ and $U-a=-1/3$) see figures 1 and 2. There are no apparent differences in the two methods used to impose the boundary conditions. The convergence rate is close to four when a wave has reached the boundary, as it should be since the overall accuracy is at most one order higher than at the boundary [5]. The same tests were done with the SBP operator of second order with similar results.

Different time steps were also used with the high order SBP operator, varying from $CFL = 0.1$ and $CFL = 0.99$. If a larger CFL number was used the convergence rate dropped somewhat but not below four when the waves were inside the domain and then dropped to about four at the boundary.

Since we have a sixth order stencil in the interior we should expect sixth order accuracy until a wave reaches the boundary, and one explanation may be that the initial condition has a discontinuous derivative.

Some wiggles were observed in the solution see section 7.3, these can be damped using artificial dissipation. This is often necessary when using finite difference methods with no inherent dissipation as with the present SBP operators.

The time instants were chosen such that for the first time both waves were inside the computational domain, for the second time $t = 0.75$ one had reached the boundary and in the last case the first wave had left the domain and the second had reached the other boundary. In some test runs the computation continued until $T = 20$ to check for long time stability. Some small wiggles were observed in the solution due to the fact that no artificial dissipation was added to the numerical scheme, and also due to the fact that the initial condition has a discontinuous first derivative. In more realistic test cases artificial dissipation has to be added to damp high frequency oscillations.

Results using the projection method can be seen in table 1. The convergence rate is computed with respect to a grid with half as many points. The columns give the results from three time instants 0.25, 0.75 and 1.5.

Table 1: Order of accuracy for SBP 3-6 using the projection method for the isentropic Euler equations

| # of grid points / Time | 0.25 | 0.75 | 1.5 |
|-------------------------|--------|--------|--------|
| 100 | | | |
| 200 | 4.7253 | 4.0004 | 3.9834 |
| 400 | 4.4069 | 4.0140 | 4.0369 |
| 800 | 4.2376 | 4.0138 | 4.0453 |

Results using the simultaneous approximation term method can be seen in table 2. The convergence rate is computed with respect to a grid with half as many points. The columns give the results from three time instants 0.25, 0.75 and 1.5.

Table 2: Order of accuracy for SBP 3-6 using the simultaneous approximation term method for the isentropic Euler equations

| # of grid points / Time | 0.25 | 0.75 | 1.5 |
|-------------------------|--------|--------|--------|
| 100 | | | |
| 200 | 4.7253 | 4.0004 | 3.9885 |
| 400 | 4.4069 | 4.0140 | 4.0779 |
| 800 | 4.2376 | 4.0138 | 4.0961 |

For both the projection and SAT method we observe an overall forth order accuracy, as should be expected. More surprising is that the order of accuracy is not close to six when no wave has reached the boundary. Later experiments indicated that reason for the lower accuracy was caused by the non-smooth initial condition, cf. section 7.3.

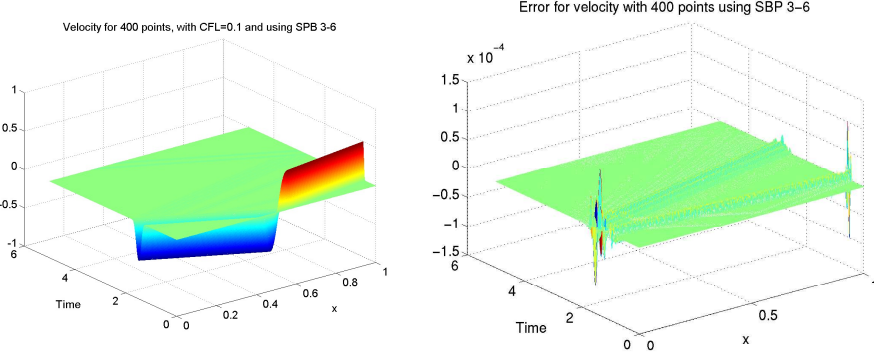


Figure 1: Acoustic velocity and error fields for the isentropic linearized 1D Euler equations using 400 points in the x -direction.

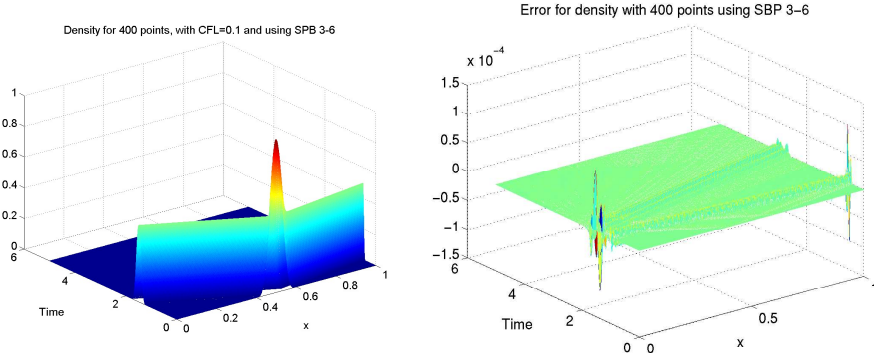


Figure 2: Density perturbations and error fields for the isentropic linearized 1D Euler equations using 400 points in the x -direction.

The large errors observed at the boundaries in figures 1 and 2 were unexpected, because one had expected an error at the boundary that was comparable to the error inside the computational domain. Future investigation will deal with this problem.

7.2 Non-isentropic test case

7.2.1 Left going acoustic wave

The initial values are now instead given by

$$u'(x, 0) = \alpha e^{(-\beta(x-0.5)^2)} \quad (35)$$

$$p'(x, 0) = -R u'(x, 0) \quad (36)$$

$$\rho'(x, 0) = -R u'(x, 0)/a \quad (37)$$

where the parameters are chosen as $\alpha = 1$ and $\beta = 250$. The Mach number is chosen to be 0.5.

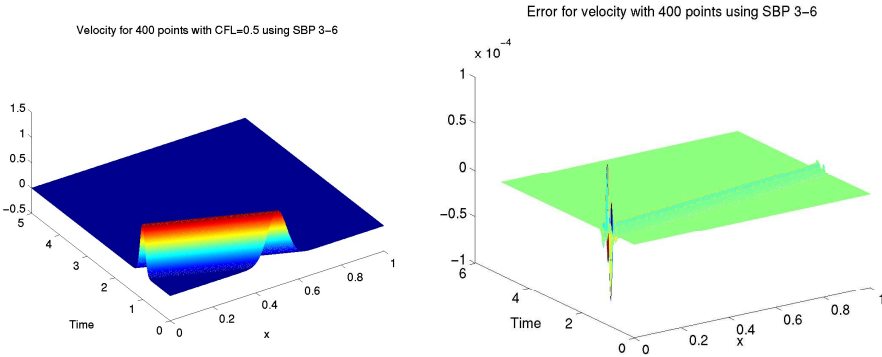


Figure 3: Acoustic velocity end error fields for the non isentropic linearized 1D Euler equation using 400 points in the x -direction, respectively.

The wave in figure 3 is moving to the left and therefore corresponds to the eigenvalue $U - a$. The only Riemann invariant that is non zero with the initial values used is the one corresponding to the same eigenvalue. The characteristic variables are given by multiplying the primitive variables i.e. ρ, u , and p with the inverse of the eigenvector matrix from the left.

Table 3: Order of accuracy for SBP 3-6 using the simultaneous approximation term method for the non-isentropic Euler equations, with left going acoustic wave.

| # of grid points /Time | 0.25 | 0.75 | 1.5 |
|------------------------|--------|--------|--------|
| 100 | | | |
| 200 | 5.8772 | 5.7965 | 3.9386 |
| 400 | 5.8238 | 5.7486 | 3.9602 |
| 800 | 5.6634 | 5.5458 | 3.9678 |

In table 3 the time instants 0.25, 0.75 and 1.5 were the same as for the isentropic case for convenience. For the first two time instants the wave is still inside the domain, and has left at the third. Now we observe about sixth order of accuracy, when no information has reached the boundary as we should expect.

7.2.2 Right going acoustic wave

The initial values are now given by

$$u'(x, 0) = \alpha e^{(-\beta(x-0.5)^2)} \quad (38)$$

$$p'(x, 0) = Rau'(0, x) \quad (39)$$

$$\rho'(x, 0) = Ru'(x, 0)/a \quad (40)$$

where the parameters are chosen as, $\alpha = 1$ and $\beta = 250$. The Mach number is chosen to be 0.5.

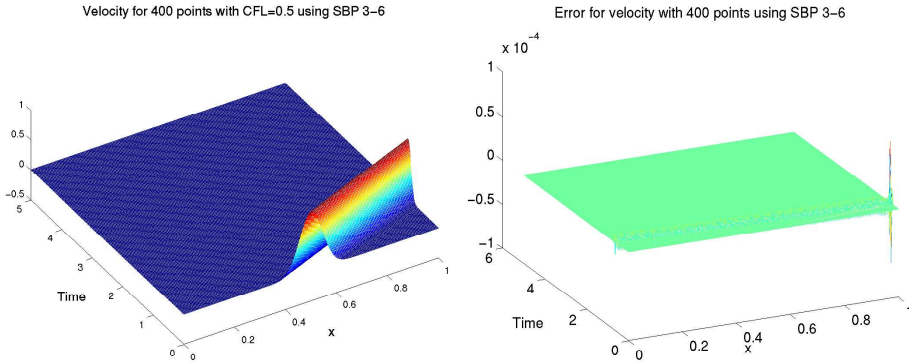


Figure 4: Acoustic velocity and error fields for the non isentropic linearized 1D Euler equation using 400 points in the x -direction, respectively.

The wave in figure 4 is moving to the right and therefore corresponds to the eigenvalue $U + a$. The only Riemann invariant that is non zero with the initial values used is the one corresponding to the same eigenvalue.

Table 4: Order of accuracy for SBP 3-6 using the simultaneous approximation term method for the non-isentropic Euler equations, with right going acoustic wave.

| # of grid points /Time | 0.05 | 0.15 | 0.3 |
|------------------------|--------|--------|--------|
| 100 | | | |
| 200 | 5.9284 | 5.9189 | 3.9354 |
| 400 | 5.9424 | 5.9353 | 3.9585 |
| 800 | 5.8441 | 5.8203 | 3.9667 |

The reason for using different time instants was the greater speed of the right going wave. So in order to capture it inside the domain smaller time instants had to be used. At the first two time instants 0.05 and 0.15 the wave is still inside the domain and at the last instant 0.3 it has left the computational domain.

As before we compare the numerical solution with the exact solution and the results are similar to the isentropic case. Except of course the observed close to sixth order accuracy when the wave was still inside the domain cf. table 4.

7.2.3 Right going entropy wave

The initial values are now given by

$$u'(x, 0) = 0 \quad (41)$$

$$p'(x, 0) = 0 \quad (42)$$

$$\rho'(x, 0) = \alpha e^{(-\beta(x-0.5)^2)} \quad (43)$$

$$(44)$$

where the parameters are chosen as $\alpha = 1$ and $\beta = 250$. The Mach number is chosen to be 0.5. For the above initial conditions only the density ρ' is non zero.

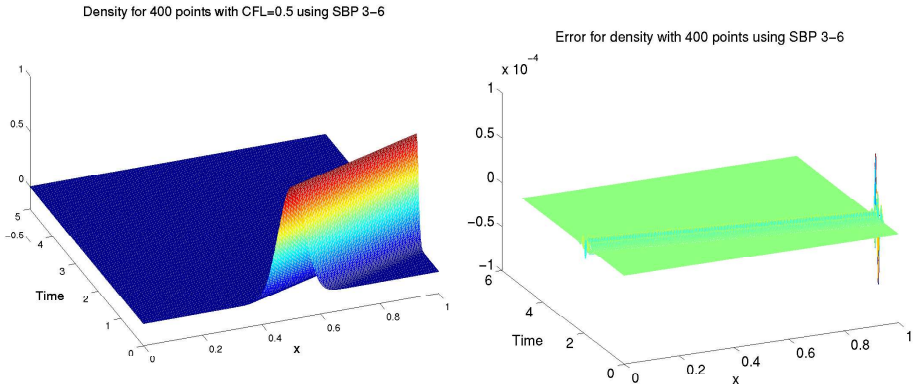


Figure 5: Acoustic density and error fields for the non isentropic linearized 1D Euler equation using 400 points in the x -direction, respectively.

Table 5: Order of accuracy for SBP 3-6 using the simultaneous approximation term method for the non-isentropic Euler equations, with right going entropy wave.

| # of grid points /Time | 0.25 | 0.75 | 1.5 |
|------------------------|--------|--------|--------|
| <hr/> | | | |
| 200 | 5.9243 | 5.9148 | 4.0473 |
| 400 | 5.9324 | 5.9253 | 4.0852 |
| 800 | 5.8960 | 5.8899 | 4.0885 |

In the above experiment see figure 5 and table 5, we have chosen the initial condition such that only one Riemann invariant, namely entropy, was non-zero.

All three test cases for the non-isentropic Euler equations displayed sixth order accuracy and fourth order when the wave reaches the boundary as theory predicts. Also the wiggles that were observed in the isentropic case with the non-smooth initial condition were not observed and are discussed in the following section.

7.3 Comparison between \mathcal{C}^0 and \mathcal{C}^∞ initial data

For the isentropic case the following \mathcal{C}^0 initial data was used cf. figure 6

$$u'(x, 0) = \begin{cases} (\sin \frac{x-0.4}{0.2}\pi)^4 & \text{if } 0.4 \leq x \leq 0.6 \\ 0 & \text{otherwise.} \end{cases}$$

and the initial density perturbation ρ' is set to zero. As before the Mach number $M = U/a$ was chosen to be 0.5.

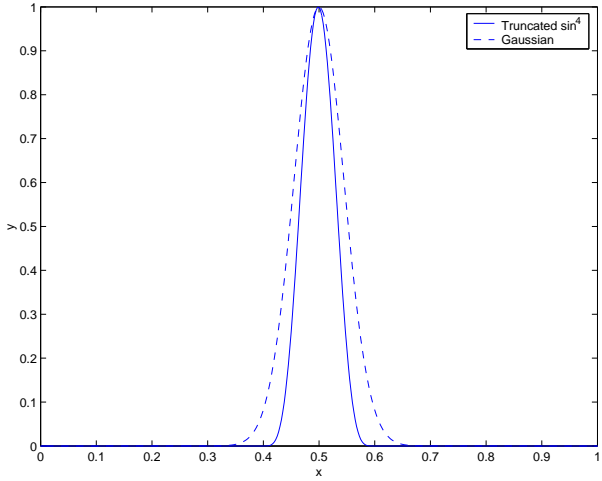


Figure 6: The two initial conditions, solid for the truncated \sin^4 curve and dashed for the Gaussian curve.

Due to the discontinuity in the first derivative there are wiggles in the solution as can be seen in Fig. 7. The discontinuity leads to high frequency oscillations in the Fourier domain that cannot be represented by the finite difference method.

These wiggles are not present when we use the \mathcal{C}^∞ initial data that were used in the non isentropic case

$$u'(x, 0) = \alpha e^{(-\beta(x-0.5)^2)}$$

with $\alpha = 250$ and $\beta = 0.5$.

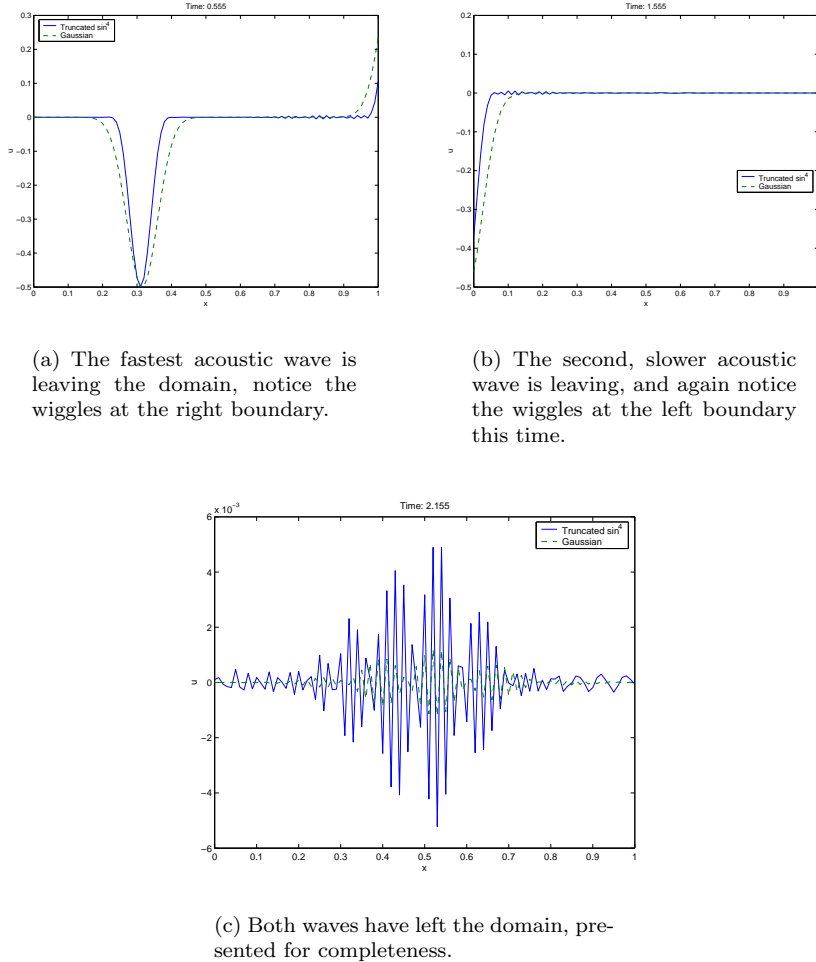


Figure 7: Numerical solution using different initial data, solid denotes the one with truncated \sin^4 and dashed the Gaussian curve.

We have seen the high frequency oscillations that occur in the numerical solution when using the truncated \sin^4 curve as initial condition. These oscillations are most likely the cause of the fact that sixth order accuracy was not observed when no wave had reached the boundary in the isentropic case.

7.4 Comparison between SBP 1-2 and SBP 3-6

The summation by parts operator SBP 3-6 has third order accuracy at the boundary and therefore the overall accuracy is fourth order[5]. The SBP 1-2 operator therefore is of second order accuracy, the figures 8 and 9 show the error compared to the exact solution.

The time to solve the non isentropic Euler equations using with SBP 3-6 is only about 50 % more per time step than with SBP 1-2, and the figure 8 shows the advantage of the high order method on this case.

For the SBP 3-6, the error is about one order of magnitude smaller until the wave reaches the boundary where the error has a jump. When the wave leaves the boundary the accuracy is not sixth order as it was in the interior but fourth order.

When using the SBP 1-2 it is also apparent that the error grows linearly with time, this can also be seen when zooming in on 9. This can be observed with all finite difference methods.

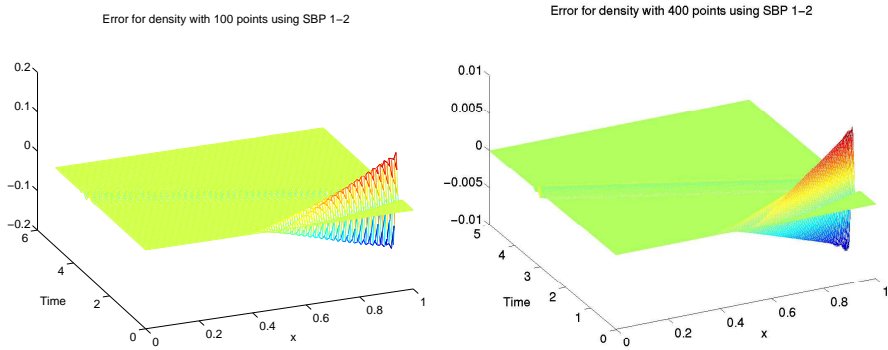


Figure 8: The error with time for the density with 100 and 400 points using SBP 1-2.

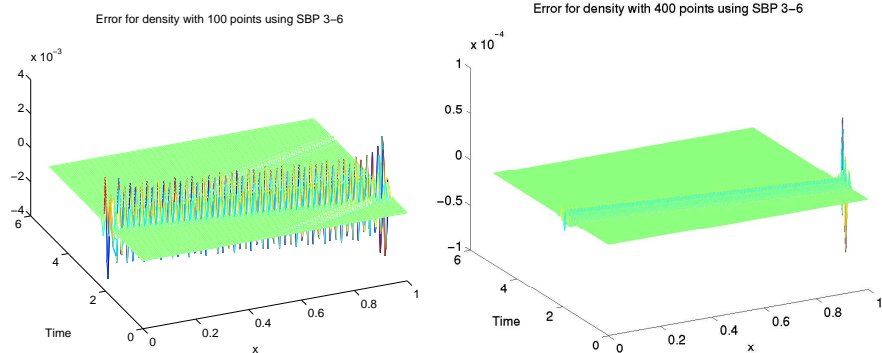


Figure 9: The error with time for the density with 100 and 400 points using SBP 3-6.

7.4.1 Mach number dependence

In order to investigate the Mach number dependence on the numerical solution a test case was chosen with Mach number equal to 0.1. The initial values are

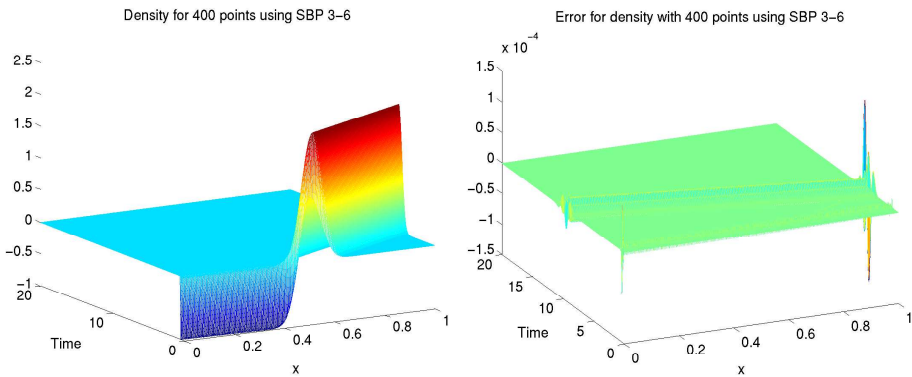
now given by

$$u'(x, 0) = \alpha e^{(-\beta(x-0.5)^2)} \quad (45)$$

$$p'(x, 0) = -\alpha e^{(-\beta(x-0.5)^2)} \quad (46)$$

$$\rho'(x, 0) = \alpha e^{(-\beta(x-0.5)^2)} \quad (47)$$

where the parameters are chosen as $\alpha = 1$ and $\beta = 250$.



In the previous test cases for the non-isentropic Euler equations there are now three waves present a left and a right going acoustic wave and a right going entropy wave.

The same behaviour is observed as for the three test cases for the linear non-isentropic Euler equations with Mach number 0.5. That is that there are some problems at the boundaries which were not anticipated. Other then that the only difference is that the calculations must be run for longer time in order to let the slowest wave leave the domain, namely the entropy wave.

8 Conclusions

The summation by parts operators of overall fourth order are used together with the projection method and the simultaneous approximation term method to implement the boundary conditions and the classical fourth order Runge-Kutta method for time-stepping. The isentropic linearized 1D Euler equations and the non isentropic linearized 1D Euler equations are considered. Note that the projection method was not used for the non isentropic linearized Euler equations.

No noticeable differences were observed between the projection or simultaneous approximation term method, neither in accuracy or time to solve the problem for the isentropic linearized Euler equations.

A comparison between summation by parts operators with different orders of accuracy showed that a 50 % increase in computation time for the high order method reduced the error by about two orders magnitude compared with the second-order method.

The errors of the reflected numerical waves are considerably larger then the errors of the outgoing physical waves. These problems at the boundary

that were observed with the high order method were not anticipated. However, when the same method and boundary conditions were implemented for the scalar Kreiss equation, the same problem at the boundary was found. One possible explanation of the problem is that the discrete method allows for unphysical waves traveling in the wrong direction, which the boundary conditions will not handle properly. Further investigations will be conducted to determine the source of the problem.

9 Appendix

The SBP operator with sixth order accuracy in the interior and third near the boundary (SBP 3-6) has a standard centered finite difference operator in the interior of \mathbf{D}

$$\begin{aligned} D(j, j - 3) &= -\frac{1}{60h}, \quad D(j, j - 2) = \frac{3}{20h}, \quad D(j, j - 1) = -\frac{3}{4h}, \\ D(j, j) &= 0, \quad D(j, j + 1) = \frac{3}{4h}, \quad D(j, j + 2) = -\frac{3}{20h}, \\ D(j, j + 3) &= \frac{1}{60h} \quad \text{for } j = 7, \dots, N - 6 \end{aligned}$$

\mathbf{H} is a diagonal matrix with ones in the diagonal except for some elements in the beginning and end of the diagonal. In this case the first ones read 13649/43200 12013/8640 2711/4320 5359/4320 7877/8640 and 43801/43200, and in reverse order at the end.

Below is the boundary operator for \mathbf{D} in the SBP 3-6 operator, namely $\mathbf{D}(1:6, 1:9) = \mathbf{Q}/h$. The indices refer to indices in \mathbf{D} but the same operator is located in the bottom right half corner with opposite sign and the elements are in a different order as the MATLAB code shows.

$\mathbf{D}(N-5:N, N-8:N) = -\mathbf{Q}(6:-1:1, 9:-1:1)/h;$

$$\begin{aligned} Q(1, 1) &= -1.5825335189391164188 \\ Q(1, 2) &= 1.9968007424231323418 \\ Q(1, 3) &= .47988863653014872884 * 10^{-2} \\ Q(1, 4) &= -.66986592424353432486 \\ Q(1, 5) &= .25079981439421691455 \\ Q(1, 6) &= 0 \\ Q(1, 7) &= 0 \\ Q(1, 8) &= 0 \\ Q(1, 9) &= 0 \\ Q(2, 1) &= -.45374732928216654180 \\ Q(2, 2) &= 0 \\ Q(2, 3) &= .20413995948833208469 \\ Q(2, 4) &= .42505341435666916396 \\ Q(2, 5) &= -.19379006076750187297 \\ Q(2, 6) &= .18344016204667166126 * 10^{-1} \\ Q(2, 7) &= 0 \\ Q(2, 8) &= 0 \\ Q(2, 9) &= 0 \\ Q(3, 1) &= -.24160826263371449650 * 10^{-2} \end{aligned}$$

$Q(3, 2) = -0.45229312676749047092$
 $Q(3, 3) = 0$
 $Q(3, 4) = 0.23791958686831427518$
 $Q(3, 5) = 0.34541374646501905816$
 $Q(3, 6) = -0.12862412393950571745$
 $Q(3, 7) = 0$
 $Q(3, 8) = 0$
 $Q(3, 9) = 0$
 $Q(4, 1) = 0.17061018846799776078$
 $Q(4, 2) = -0.47641039995023947254$
 $Q(4, 3) = -0.12035827579772345587$
 $Q(4, 4) = 0$
 $Q(4, 5) = 0.42710082726876904895$
 $Q(4, 6) = -0.14377682403433476395 * 10^{-1}$
 $Q(4, 7) = 0.13435342414629595074 * 10^{-1}$
 $Q(4, 8) = 0$
 $Q(4, 9) = 0$
 $Q(5, 1) = -0.86915492361728238331 * 10^{-1}$
 $Q(5, 2) = 0.29554398882823409928$
 $Q(5, 3) = -0.23775972239854428505$
 $Q(5, 4) = -0.58114341331302103170$
 $Q(5, 5) = 0$
 $Q(5, 6) = 0.75652321103635055647$
 $Q(5, 7) = -0.16452964326520248826$
 $Q(5, 8) = 0.18281071473911387584 * 10^{-1}$
 $Q(5, 9) = 0$
 $Q(6, 1) = 0$
 $Q(6, 2) = -0.25155437851495019140 * 10^{-1}$
 $Q(6, 3) = 0.79610054564964270222 * 10^{-1}$
 $Q(6, 4) = 0.17590922581676217438 * 10^{-1}$
 $Q(6, 5) = -0.68025083141176381057$
 $Q(6, 6) = 0$
 $Q(6, 7) = 0.73970913906075203762$
 $Q(6, 8) = -0.14794182781215040752$
 $Q(6, 9) = 0.16437980868016711947 * 10^{-1}$

References

- [1] M. Billson, L.-E. Eriksson, and L. Davidson. Acoustics Source Terms for the Linear Euler Equations on Conservative Form. AIAA Paper, 2002-2582, 2002.
- [2] M.H. Carpenter, D. Gottlieb, and S. Abarbanel. Time-Stable Boundary Conditions for Finite-Difference Schemes Solving Hyperbolic Systems: Methodology and Application to High-Order Compact Schemes. *J. Comp. Phys.*, 111:220–236, (1994).
- [3] G. Dahlquist and Å. Björck. *Numerical Methods*. Prentice-Hall, 1974.
- [4] Crighton D.G. Computational Aeroacoustics For Low Mach Number Flows. In J.C. Hardin and M.Y. Hussaini, editors, *Computational Aeroacoustics*, ICASE/NASA LaRC Series, 1995.
- [5] B. Gustafsson. The Convergence Rate for Difference Approximations to Mixed Initial Boundary Value Problems. *Math. Comp.*, 29(130):396–406, (1975).
- [6] H.-O. Kreiss and G. Scherer. Finite Element and Finite Difference Methods for Hyperbolic Partial Differential Equations. In C. De Boor, editor, *Mathematical Aspects of Finite Elements in Partial Differential Equations.*, pages 195–211. Academic Press, Inc., (1974).
- [7] J. Lighthill. On sound generated aerodynamically. I. General theory. *Proc. of the Royal Soc. of London A*, 211:564–587, (1952).
- [8] P. Olsson. Summation by Parts, Projections, and Stability. I. *Math. Comp.*, 64:1035–1065, (1995).
- [9] L.F. Richardson. The Approximate Arithmetical Solution by Finite Differences of Physical Problems involving Differential Equations, with an Application to the Stresses in a Masonry Dam. *Philo. Trans. of the Royal Soc. of London*, 210:307–357, (1910).
- [10] B. Strand. Summation by Parts for Finite Difference Approximations for d/dx . *J. Comp. Phys.*, 110:47–67, (1994).
- [11] C.K.W Tam. Computational aeroacoustics: Issues and methods. *AIAA J.*, 33:1788–1796, (1995).

Paper B

HIGH ORDER FINITE DIFFERENCE OPERATORS WITH THE SUMMATION BY PARTS PROPERTY BASED ON DRP SCHEMES

Stefan Johansson

Division of Scientific Computing
Department of Information Technology
Uppsala University
P.O. Box 337
SE 75105 Uppsala
Sweden

Abstract.

Strictly stable high order finite difference methods based on Tam and Webb's dispersion relation preserving schemes have been constructed. The methods have been implemented for a 1D hyperbolic test problem, and the theoretical order of accuracy is observed.

1 Introduction

Computational aeroacoustics (CAA) has been given increased interest because of the need to better control noise levels from aircrafts, trains, cars, etc. due to increased transport and stricter regulations from authorities. Other applications range from simulating sound propagation in the atmosphere to improved design of musical instruments.

Much of the current effort in CAA involves the development of schemes for approximating derivatives in a way that better preserves the physics of wave propagation, a phenomenon of less significance in typical aerodynamic computations. An example of such a scheme is the Dispersion Preserving Relation (DRP) scheme proposed by Tam and Webb [5].

In scientific computing it is imperative that the numerical methods are stable. A good approximation of the wave propagation requires high order methods and for difference methods problems arise when applying boundary conditions. To accurately prescribe boundary conditions the simultaneous approximation term (SAT) method [1] can be used if the space derivatives are discretized by a summation by parts (SBP) operator proposed by Kreiss and Scherer [3].

In this paper SBP operators are derived for DRP type schemes, which together with the SAT method lead to strictly stable methods.

2 Theory

In recent years, central difference methods of the type proposed by Tam and Webb [5] called Dispersion Preserving Relation schemes (DRP) have attracted interest in aeroacoustics. The formal accuracy of the method is lowered to get a better approximation of the wave number.

Another development in the theory of finite difference methods is high order operators $Q = \frac{1}{h} H^{-1} B$ with the summation by parts property (SBP) developed by Strand [4], i.e. $B + B^T = \text{diag}(-1, 0, \dots, 0, 1)$, with a discrete norm H and step size h . A consequence is that a stability proof done by the energy method for the continuous problem is valid for the semi-discrete problem if a SBP operators are used.

What we have done is to construct a SBP operator for difference schemes of DRP type. The motivation has been to combine the good wave resolution of DRP schemes with the good stability properties of SBP operators when using using SAT to prescribe boundary conditions in a strictly stable way, first shown by Carpenter et al. [1].

Consider the discrete function v approximating the continuous function u on $\{x_j\}_0^N$ where $x_j = hj$, $h = 1/N$ and let v_j denote $v(x_j)$. A classical central finite difference method approximating du/dx at x_m is

$$(Qv)_j = \frac{1}{h} \sum_{j=1}^l \alpha_j (v_{m+j} - v_{m-j}) \quad (2.1)$$

where α_k , $k = 1 \dots l$ are chosen such that the accuracy is of order $2l$.

Tam and Webb [5] proposed that the accuracy is lowered to $2(l-1)$ leaving a free parameter and then minimize the wave number error

$$\int_{-\pi/2}^{\pi/2} |hk - h\tilde{k}|^2 d(hk) \quad (2.2)$$

where k and \tilde{k} are the exact and the approximate wave numbers, respectively.

A comparison between standard centered finite difference methods and DRP schemes is given in figure 2.1. Noticeable is that the fourth order DRP scheme derived from a sixth order standard scheme approximates the wave number about as well as the eighth order standard scheme. In figure 2.2 it can be seen that the DRP schemes in an interval near $kh = 1$ lies strictly above the line defining the exact group velocity. The approximation of the wave number and group velocity can be improved for $hk < 2$ by choosing a larger interval to optimize over in equation 2.2, at the expense of a poorer approximation for $kh > 2$.

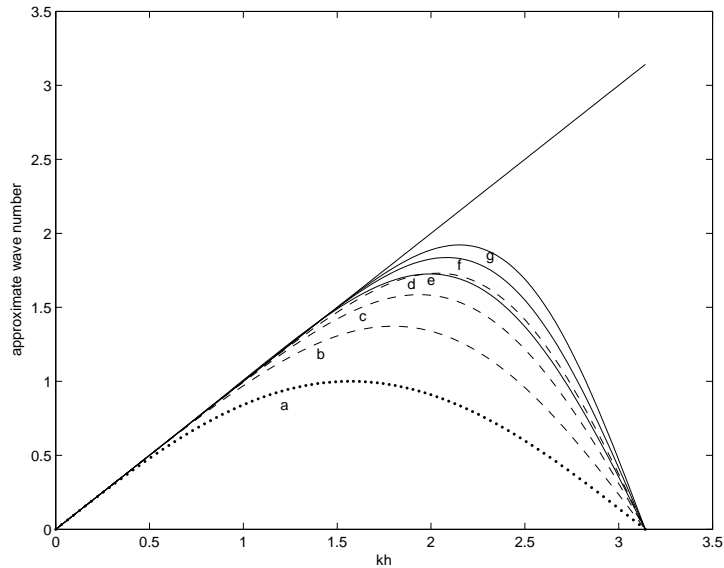


Figure 2.1: Approximate wave number vs exact for 2nd order standard centered difference method (SC2) (a) (dotted), SC4 (b), SC6 (c), SC8 (d) (dashed) and DRP schemes with order four (e) six (f) and eight (g) (solid).

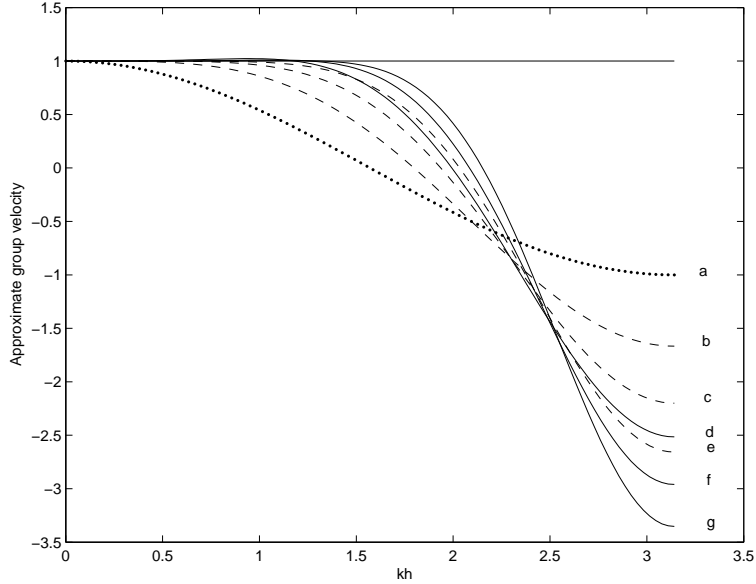


Figure 2.2: Approximate group velocity vs exact for 2nd order standard centered difference method (SC2) (a) (dotted), SC4 (b), SC6 (c), SC8 (d) (dashed) and DRP schemes with order four (e) six (f) and eight (g) (solid).

3 Summation by Parts Operators

When doing numerical calculations, we must establish an upper bound on the growth of the solution. In the continuous case the energy method is often used, for example, with the usual L_2 scalar product and norm

$$(u, v) = \int_0^1 uv \, dx, \quad \|u\| = (u, u)^{1/2}. \quad (3.1)$$

We have for the simplest hyperbolic equation, sometimes called the Kreiss equation,

$$\begin{cases} u_t &= u_x, \quad x \in [0, 1], t \geq 0 \\ u(x, 0) &= f(x), \quad x \in [0, 1] \\ u(1, t) &= g(t) \quad t \geq 0 \end{cases} \quad (3.2)$$

the following energy growth

$$\frac{1}{2} \frac{d\|u\|^2}{dt} = (u, u_t) = (u, u_x) = \int_0^1 uu_x \, dx = \frac{1}{2}[u^2]_0^1 = \frac{1}{2}(g(t)^2 - u(0, t)^2) \quad (3.3)$$

If $g \equiv 0$ it follows that $\|u\| \leq \|f\|$ and the problem is well posed.

In the discrete case we want to find an operator Q that in a modified norm, determined by H , gives the same estimate as the continuous case. That is Q must satisfy

$$(u, Qv)_h = u_n v_n - u_0 v_0 - (Qu, v)_h \quad (3.4)$$

where

$$(u, v)_h = h u^T H v. \quad (3.5)$$

The matrix Q is a banded matrix where row j approximate $\frac{du_j}{dx}$. Of course Q has to be modified at the l first and l last rows, where l is equal to or larger than the bandwidth of Q . The matrix H is a modified identity matrix, its l first elements are modified.

Since equation (3.4) is the discrete analogue of integration by parts, it is called the summation by parts property.

An example of such an operator Q and scalar product H is

$$Q = \frac{1}{h} \begin{pmatrix} -1 & 1 & 0 & \dots & 0 \\ -0.5 & 0 & 0.5 & \ddots & \vdots \\ 0 & \ddots & \ddots & \ddots & 0 \\ \vdots & \ddots & -0.5 & 0 & 0.5 \\ 0 & \dots & 0 & -1 & 1 \end{pmatrix}, H = \begin{pmatrix} 0.5 & 0 & \dots & 0 \\ 0 & 1 & 0 & \dots \\ \vdots & \ddots & \ddots & \ddots \\ 0 & 1 & 0 & \dots \\ 0 & \dots & 0 & 0.5 \end{pmatrix}.$$

Operators of this kind were described by Kreiss and Scherer [3], and high order operators were later constructed by Strand [4]. High order operators Q have the following structure: in the interior a centered high order finite difference stencil is used and near the boundary where the stencil cannot be used, a small dense matrix is used instead.

Given a DRP scheme of order 2τ with coefficients α_j , $j = 1 \dots \tau + 1$ a summation by parts operator Q which is accurate of order τ near the boundary and a diagonal norm matrix H with property that $h(HQ + (HQ)^T) = \text{diag}(-1, 0, \dots, 0, 1)$ will be derived.

For simplicity we approximate $\frac{d}{dx}$ for $x = [0, \infty)$ and let $h = 1$. The difference operator Q has to be modified for rows $1 \dots 2\tau$.

$$\begin{pmatrix} q_{0,0} & q_{0,1} & \dots & q_{0,2\tau-1} \\ q_{1,0} & 0 & \ddots & \vdots & q_{\tau-1,2\tau} & 0 & \dots \\ \vdots & \ddots & \ddots & q_{2\tau-2,2\tau-1} & \vdots & \ddots & 0 & \dots \\ q_{2\tau-1,0} & \dots & q_{2\tau-1,2\tau-2} & 0 & q_{2\tau-1,2\tau} & \dots & q_{2\tau-1,3\tau} & 0 & \dots \end{pmatrix}$$

In order for HQ to be nearly antisymmetric and have the SBP property the following relation must hold

$$\begin{aligned} h_{0,0}q_{0,0} &= -1/2 \\ h_{i,i}q_{i,j} &= -h_{j,j}q_{j,i} \quad 0 \leq i < 2\tau - 1 \quad i < j \leq 2\tau - 1 \\ h_{i,i}q_{i,j} &= \alpha_{j-i} \quad \tau - 1 \leq i < 2\tau \quad 2\tau \leq j \leq \tau + i + 1 \end{aligned}$$

and τ th order accuracy near the boundary leads to the following system of equations, $j = 0, \dots, \tau$. Note that $q_{i,i} = 0$ for $i \neq 0$

$$\begin{aligned} 0^j q_{0,0} + \dots + \alpha^j q_{0,\alpha} &= j * 0^{j-1} \\ \vdots &\vdots \\ 0^j q_{\beta,0} + \dots + \alpha^j q_{\beta,\alpha} &= j * \beta^{j-1} \\ \vdots &\vdots \\ 0^j q_{\gamma,0} + \dots + \gamma^j q_{\gamma,\gamma} + \dots + (3\tau)^j q_{\gamma,3\tau} &= j * \gamma^{j-1} \end{aligned}$$

where $\alpha = \max\{2, 2\tau - 1\}$, $\beta = \max\{0, \tau - 2\}$, $\gamma = 2\tau - 1$ and $j = 0, \dots, \tau$, note that $q_{i,i} = 0$ for $i \neq 0$. The accuracy conditions come from requiring that polynomials of degree τ and lower are exactly differentiated.

From these systems of equations, a system of equations with $h_{i,i}q_{i,j}$, $j > i$, $i = 0, \dots, 2(\tau - 1)$ as unknowns can be derived. The solution is used to compute $h_{i,i}$, $i = 0, \dots, 2\tau - 1$, which is used to compute $q_{i,j}$, $i = 0, \dots, 2\tau - 1$, $j = 0, \dots, 3\tau$.

To illustrate the derivation of H and Q we let $\tau = 1$. Then the following conditions yield the SBP property.

$$\begin{cases} h_{0,0}q_{0,0} &= -\frac{1}{2} \\ h_{0,0}q_{0,1} + h_{1,1}q_{1,0} &= 0 \\ h_{0,0}q_{0,2} - \alpha_2 &= 0 \\ h_{1,1}q_{1,2} - \alpha_1 &= 0 \\ h_{1,1}q_{1,3} - \alpha_2 &= 0 \end{cases} \quad (3.6)$$

First order accuracy near the boundary leads to two equation systems

$$\begin{cases} q_{0,0} + q_{0,1} + q_{0,2} = 0 \\ q_{1,0} + q_{1,2} + q_{1,3} = 0 \end{cases} \quad (3.7)$$

$$\begin{cases} q_{0,1} + 2q_{0,2} = 1 \\ 2q_{1,2} + 3q_{1,3} = 1 \end{cases} \quad (3.8)$$

Using the conditions for antisymmetry of HQ and multiplying the first equation in each system by $h_{0,0}$ and the second equation by $h_{1,1}$ yields,

$$\begin{cases} -\frac{1}{2} + h_{0,0}q_{0,1} + h_{0,0}q_{0,2} = 0 \\ -h_{0,0}q_{0,1} + \alpha_1 + \alpha_2 = 0 \end{cases} \quad (3.9)$$

$$\begin{cases} h_{0,0}q_{0,1} + 2h_{0,0}q_{0,2} = h_{0,0} \\ 2\alpha_1 + 3\alpha_2 = h_{1,1} \end{cases} \quad (3.10)$$

Using that $\alpha_1 = 1/2 - 2\alpha_2$, which is equivalent to requiring that the interior scheme is second order accurate, the solution can be computed.

$$h_{0,0} = \frac{1}{2} + \alpha_2, h_{1,1} = 1 - \alpha_2 \quad (3.11)$$

$$\begin{aligned} q_{0,0} &= -\frac{1}{1+2\alpha_2} & q_{0,1} &= \frac{1/2-\alpha_2}{h_{0,0}} & q_{0,2} &= \frac{\alpha_2}{h_{0,0}} \\ q_{1,0} &= \frac{\alpha_2-1/2}{h_{1,1}} & q_{1,1} &= 0 & q_{1,2} &= \frac{\alpha_1}{h_{1,1}} & q_{1,3} &= \frac{\alpha_2}{h_{1,1}} \end{aligned} \quad (3.12)$$

For $\tau > 2$ the system of equations for HQ is undetermined thus leading to free parameters, one for $\tau = 3$ and three for $\tau = 4$. The free parameters were initially chosen such that the bandwidth of Q was minimized, but as is seen in figure 3.1 the spectral radius for the fourth order method is very large and leads to a restrictive CFL condition. The spectral radius of Q can be made smaller if the three parameters are chosen as $[0.502, -0.1, 0.799]$, which are close to the values that minimize the bandwidth. These values were found by trial and error.

The eigenvalues in figure 3.1 were computed using MATLAB, and a computation in exact arithmetic using MAPLE showed that all eigenvalues are imaginary for SBP-2-4(6). Computations for the other SBP operators were unfortunately too time consuming to complete.

The original operators by Strand [4] are denoted by SBP- τ - 2τ and the new ones SBP- τ - 2τ - (σ) . The number in parenthesis denote the order of the difference method

modified for better wave approximation, in this article $\sigma = 2(\tau + 1)$. The operators that have been derived are SBP-1-2(4), SBP-2-4(6) SBP-3-6(8) and SBP-4-8(10), where Tam and Webb's DRP scheme corresponds to SBP-2-4(6) in the interior. They can be found in the appendix.

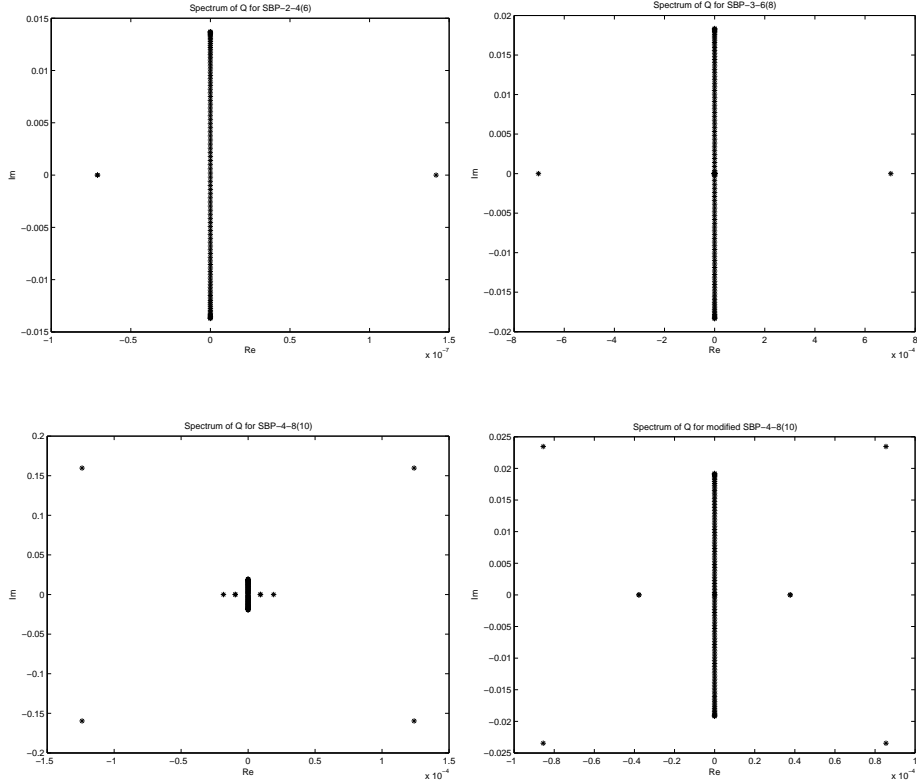


Figure 3.1: Spectrum for SBP-2-4(6), SBP-3-6(8), SBP-4-8(10) and a modified SBP-4-8(10), $h = 1/100$.

4 Numerical experiments

The summation by parts operators for DRP schemes were tested for the hyperbolic system

$$u_t + \begin{pmatrix} 1 & 0 \\ 0 & -1 \end{pmatrix} u_x = 0, \quad u = \begin{pmatrix} u^I \\ u^{II} \end{pmatrix}, \quad 0 \leq x \leq 1, \quad t \geq 0,$$

With the initial data

$$u^I(x, 0) = \sin 2\pi x, \quad u^{II}(x, 0) = -\sin 2\pi x, \quad 0 \leq x \leq 1,$$

and boundary conditions

$$u^I(0, t) = u^{II}(0, t), \quad u^{II}(1, t) = u^I(1, t), \quad t \geq 0,$$

the exact solution is

$$u^I = \sin 2\pi(x - t), \quad u^{II} = -\sin 2\pi(x + t).$$

The boundary conditions were imposed using the simultaneous approximation term (SAT) method [1].

In the SAT method one does not impose the exact boundary conditions (b.c.) which might destroy the SBP property and therefore strict stability. Instead the boundary conditions are imposed as a penalty term at the same accuracy as the discretization.

In our case, the SAT formulation reads

$$v_t + Q \otimes \begin{pmatrix} 1 & 0 \\ 0 & -1 \end{pmatrix} v = -\frac{1}{h} H^{-1} \otimes \begin{pmatrix} 1 & 0 \\ 0 & 1 \end{pmatrix} P \quad (4.1)$$

where $v = (v_0^I, v_1^I, \dots, v_N^I, v_N^{II})^T$ denotes the numerical approximation of the exact solution u , and the matrix P which is imposing the boundary conditions and reads

$$P = \begin{pmatrix} 1 & -1 & 0 & \dots & 0 & 0 \\ 0 & 0 & & \dots & 0 & 0 \\ \vdots & \vdots & & & \vdots & \vdots \\ 0 & 0 & & \dots & 0 & 0 \\ 0 & 0 & \dots & 0 & -1 & 1 \end{pmatrix} \quad (4.2)$$

Table 4.1: Order of accuracy for u^I using SBP 2-4 and SBP 2-4(6) for the 1D test case at $t = 1.5$.

| # of grid points / | SBP 2-4 | SBP 2-4(6) |
|--------------------|---------|------------|
| 101 | | |
| 202 | 3.0134 | 3.0137 |
| 401 | 3.0091 | 3.0106 |
| 801 | 3.0068 | 3.0083 |

Table 4.2: Order of accuracy for u^I using SBP 3-6(8) for the 1D test case at $t = 1.5$.

| # of grid points / | SBP 3-6(8) |
|--------------------|------------|
| 101 | |
| 202 | 3.9141 |
| 401 | 4.1361 |
| 801 | 4.3108 |

Table 4.3: Order of accuracy for u^I using SBP 4-8(10) for the 1D test case at $t = 1.5$.

| # of grid points / | SBP 4-8(10) |
|--------------------|-------------|
| 101 | |
| 202 | 4.6758 |
| 401 | 4.6000 |
| 801 | 4.5678 |

The orders of accuracy for SBP-2-4 (SBP operator, 2nd order near boundaries, 4th order standard scheme in interior) and SBP-2-4(6) (SBP operator, 2nd order near boundaries, 4th order DRP scheme derived from 6th order standard scheme in interior) agree with theory, saying that the global order of accuracy for a finite difference scheme is at most one order higher than the accuracy at the boundaries [2].

5 Conclusions

New strictly stable high order finite difference methods have been developed. They are based on dispersion relation preserving type schemes proposed Tam and Webb [5] and strictl stability is guaranteed by requiring that the methods have the summation by parts property introduced by Kreiss and Scherer [3].

The methods have been developed using MAPLE and implemented in MATLAB. Numerical experiments show that the order of accuracy corresponds to theory.

6 Appendix

6.1 SBP operators with diagonal norm and minimal bandwidth

6.1.1 Second order at the boundary, SBP-2-4(6)

A SBP operator with a fourth order DRP finite difference operator in the interior and second order near the boundary (SBP 2-4(6)) has the following centered finite difference operator in the interior of hQ

$$\begin{aligned} hQ(j, j-3) &= -\alpha_3, & hQ(j, j-2) &= -\alpha_2, & hQ(j, j-1) &= -\alpha_1, \\ hQ(j, j) &= 0, \\ hQ(j, j+1) &= \alpha_1, & hQ(j, j+2) &= \alpha_2, & hQ(j, j+3) &= \alpha_3 \quad \text{for } j = 7, \dots, N-6 \end{aligned}$$

where α_j has the following values

$$\alpha_1 = 0.79926642697415587 \quad \alpha_2 = -0.18941314157932453 \quad \alpha_3 = 0.026519952061497799$$

H is a diagonal matrix with ones in the diagonal except for the first and last four elements of the diagonal. In this case the first four elements read

$$\begin{aligned} h_{0,0} &= 0.34532668264616756, & h_{1,1} &= 1.2556866187281647, \\ h_{2,2} &= 0.86931338127183581, & h_{3,3} &= 1.0296733173538330 \end{aligned}$$

and in reverse order for $h_{n-3,n-3}, \dots, h_{n,n}$.

Below is the boundary operator for hQ for the SBP 2-4(6) operator. The same operator is located in the bottom right half corner with opposite sign and the elements are in a different order as this MATLAB code indicates.

```
Q(N-3:N,N-6:N) = -Q(3:-1:0,6:-1:0);
```

| | |
|-----------------------------|-----------------------------|
| q00 = -1.4479043326991200 | q10 = -0.50703996036005625 |
| q01 = 1.8437129980973616 | q11 = 0 |
| q02 = -0.34371299809736176 | q12 = 0.54223976216033715 |
| q03 = -0.052095667300879370 | q13 = -0.056319682880449493 |
| q04 = 0 | q14 = 0.021119881080168560 |
| | |
| q20 = 0.13653680246090086 | q30 = 0.017471584109301608 |
| q21 = -0.78324253158386005 | q31 = 0.068681853722050198 |
| q22 = 0 | q32 = -0.70418755285702870 |
| q23 = 0.83408716489415180 | q33 = 0 |
| q24 = -0.21788821575736760 | q34 = 0.77623301828214610 |
| q25 = 0.030506779986175047 | q35 = -0.18395459840223802 |
| q26 = 0 | q36 = 0.025755695145768824 |

6.1.2 Third order at the boundary, SBP-3-6(8)

A SBP operator with a sixth order DRP finite difference operator in the interior and third order near the boundary (SBP 3-6(8)) has the following centered finite difference operator in the interior of hQ

$$\begin{aligned} hQ(j, j-4) &= -\alpha_4, & hQ(j, j-3) &= -\alpha_3, & hQ(j, j-2) &= -\alpha_2, & hQ(j, j-1) &= -\alpha_1, \\ hQ(j, j) &= 0, \\ hQ(j, j+1) &= \alpha_1, & hQ(j, j+2) &= \alpha_2, & hQ(j, j+3) &= \alpha_3 & hQ(j, j+4) &= \alpha_4 \quad \text{for } j = 9, \dots, N-8 \end{aligned}$$

where α_j has the following values

$$\begin{aligned}\alpha_1 &= 0.8331572598964345 & \alpha_2 &= -0.2331572598964345 \\ \alpha_3 &= 0.05230549233656718 & \alpha_4 &= -0.005939804278316752\end{aligned}$$

H is a diagonal matrix with ones in the diagonal except for the first and last six elements of the diagonal. In this case the first six elements read

$$\begin{aligned}h_{0,0} &= 0.3153550936462424, & h_{1,1} &= 1.393363420657677, \\ h_{2,2} &= 0.6216064920179795, & h_{3,3} &= 1.246449063537576, \\ h_{4,4} &= 0.9087199126756564, & h_{5,5} &= 1.014506017464869\end{aligned}$$

and in reverse order for $h_{n-5,n-5}, \dots, h_{n,n}$.

Below is the boundary operator for hQ for the SBP 3-6(8) operator. The same operator is located in the bottom right half corner with opposite sign and the elements are in a different order as this MATLAB code indicates.

`Q(N-5:N,N-9:N) = -Q(5:-1:0,9:-1:0);`

| | |
|--|--|
| <code>q00 = -1.585514266533103</code> | <code>q01 = 2.008723732799078</code> |
| <code>q10 = -0.4546274514421262</code> | <code>q11 = 0</code> |
| <code>q20 = 0.006638621722402879</code> | <code>q21 = -0.4773187801117445</code> |
| <code>q30 = 0.1664613995014180</code> | <code>q31 = -0.4554757153982624</code> |
| <code>q40 = -0.08600120227144731</code> | <code>q41 = 0.2769005367876363</code> |
| <code>q50 = 0</code> | <code>q42 = -0.660390739163292203649761743354</code> |
| | <code>q51 = 0.0939867209644063450256722219284</code> |
| <code>q02 = -0.0130855991986174834833673814004</code> | <code>q03 = -0.65794293386758834434421746018</code> |
| <code>q12 = 0.212941181087929195929055954261</code> | <code>q13 = 0.407450971157474941475221424938</code> |
| <code>q22 = 0</code> | <code>q14 = 0.307082033336054068764476763891</code> |
| <code>q32 = -0.153142387513228968467498042145</code> | <code>q15 = 0</code> |
| <code>q42 = -0.172627548513855444351101578662</code> | <code>q16 = 0.0148235275648283216283776183329</code> |
| <code>q52 = 0.0485326149573270703688045031784</code> | <code>q17 = 0</code> |
| <code>q04 = 0.247819066800230419419438769975</code> | <code>q18 = 0.307082033336054068764476763891</code> |
| <code>q14 = -0.180588228368106206106416068749</code> | <code>q19 = 0</code> |
| <code>q24 = 0.252362375273239592208687307356</code> | <code>q20 = -0.0792086803303361725384538561848</code> |
| <code>q34 = 0.481455867214575438317175291842</code> | <code>q21 = 0</code> |
| <code>q44 = 0</code> | <code>q22 = -0.0764973850672778007026589857013</code> |
| <code>q54 = -0.759283668722722050186941866401</code> | <code>q23 = 0.847673568210825495387209342755</code> |
| <code>q06 = 0</code> | <code>q24 = 0</code> |
| <code>q16 = 0</code> | <code>q25 = 0</code> |
| <code>q26 = -0.00955556988961586894406770497530</code> | <code>q26 = -0.229823437103968213426853599491</code> |
| <code>q36 = 0.0419636019366228644454343113704</code> | <code>q27 = 0</code> |
| <code>q46 = -0.256577694231350970143666364671</code> | <code>q28 = 0</code> |
| <code>q56 = 0.821244276084627463843621091279</code> | <code>q29 = 0</code> |
| <code>q08 = 0</code> | <code>q30 = 0</code> |
| <code>q18 = 0</code> | <code>q31 = 0</code> |
| <code>q28 = 0</code> | <code>q32 = 0</code> |
| <code>q38 = 0</code> | <code>q33 = 0</code> |
| <code>q48 = -0.00653645220651922535583776530795</code> | <code>q34 = 0</code> |
| <code>q58 = 0.0515575969349816747689080909099</code> | <code>q35 = -0.00585487338277167148733298046745</code> |

6.1.3 Fourth order at the boundary, SBP-4-8(10)

A SBP operator with a eight order DRP finite difference operator in the interior and second order near the boundary (SBP 4-8(10)) has the following centered finite difference operator in the interior of hQ

$$\begin{aligned} hQ(j, j-5) &= -\alpha_5, \quad hQ(j, j-4) = -\alpha_4, \quad hQ(j, j-3) = -\alpha_3, \\ hQ(j, j-2) &= -\alpha_2, \quad hQ(j, j-1) = -\alpha_1, \quad hQ(j, j) = 0, \\ hQ(j, j+1) &= \alpha_1, \quad hQ(j, j+2) = \alpha_2, \quad hQ(j, j+3) = \alpha_3 \\ hQ(j, j+4) &= \alpha_4, \quad hQ(j, j+5) = \alpha_5 \quad \text{for } j = 9, \dots, N-8 \end{aligned}$$

where α_j has the following values

$$\begin{aligned} \alpha_1 &= 0.85710439841851208608 \quad \alpha_2 = -0.26526216962115666981 \\ \alpha_3 &= 0.074805208507138722005 \quad \alpha_4 = -0.014448456841621349730 \\ \alpha_5 &= 0.0013596285337740972877 \end{aligned}$$

H is a diagonal matrix with ones in the diagonal except for the first and last eight elements of the diagonal. In this case the first eight elements read

$$\begin{aligned} h_{0,0} &= 0.294851829648342276, \quad h_{1,1} = 1.52599254960446488, \\ h_{2,2} &= 0.25663709986386517, \quad h_{3,3} = 1.79947333003289182, \\ h_{4,4} &= 0.411348429226366286, \quad h_{5,5} = 1.2793004001361369051, \\ h_{6,6} &= 0.9230236540992415309, \quad h_{7,7} = 1.009372707388694828 \end{aligned}$$

and in reverse order for $h_{n-7,n-7}, \dots, h_{n,n}$.

Below is the boundary operator for hQ for the SBP 4-8(10) operator. The same operator is located in the bottom right half corner with opposite sign and the elements are in a different order as this MATLAB code indicates.

`Q(N-7:N,N-12:N) = -Q(7:-1:0,12:-1:0);`

| | |
|--|---|
| <code>q00 = -1.6957669911573197987</code> | <code>q01 = 2.0621682891199350282</code> |
| <code>q10 = -0.39845154764838537791</code> | <code>q11 = 0</code> |
| <code>q20 = -1.0060547060384519478</code> | <code>q21 = 2.6156550656068261280</code> |
| <code>q30 = 0.41657226346831719539</code> | <code>q31 = -1.6072314212261918344</code> |
| <code>q40 = -1.2098265916012883296</code> | <code>q41 = 5.8230938981601276548</code> |
| <code>q50 = 0.089325888656450236921</code> | <code>q51 = -0.72026816640720284437</code> |
| <code>q60 = 0</code> | <code>q61 = 0.15057109202244840663</code> |
| <code>q70 = 0</code> | <code>q71 = 0</code> |
| <code>q02 = 0.87566342176012784417</code> | <code>q03 = -2.5423300884267936392</code> |
| <code>q12 = -0.43989345194087425217</code> | <code>q13 = 1.8952714273978855804</code> |
| <code>q22 = 0</code> | <code>q23 = -10.439577939423169752</code> |
| <code>q32 = 1.4888706386814724978</code> | <code>q33 = 0</code> |
| <code>q42 = -10.496233449667786180</code> | <code>q43 = 7.2472876183287816283</code> |
| <code>q52 = 2.0946589947956824426</code> | <code>q53 = -2.7302904871947353579</code> |
| <code>q62 = -0.70025901086696570588</code> | <code>q63 = 1.2248064281916752937</code> |
| <code>q72 = 0.017998153763907768034</code> | <code>q73 = -0.080090074114033601879</code> |

| | |
|---------------------------------|--------------------------------|
| q04 = 1.6878317108800632472 | q05 = - 0.38756634217601260433 |
| q14 = - 1.5696803558226220357 | q15 = 0.60382952310539918663 |
| q24 = 16.823791823568735151 | q25 = -10.441584991462022668 |
| q34 = - 1.6566849467542517715 | q35 = 1.9410466687451647647 |
| q44 = 0 | q45 = - 2.9362325326725905861 |
| q54 = 0.94412120877136880657 | q55 = 0 |
| q64 = - 0.83167376571312553306 | q65 = - 0.48635033688049237125 |
| q74 = 0.10696008003992586465 | q75 = 0.097204485324945230782 |
| q06 = 0 | q07 = 0 |
| q16 = -0.091075595091402694223 | q17 = -0.070788070790662511317 |
| q26 = 2.5185588185387488660 | q27 = 0.044924664119343000785 |
| q36 = -0.62825343729493118302 | q37 = -0.26246018679458559520 |
| q46 = 1.8661905666948906603 | q47 = -0.076694695407211351188 |
| q56 = 0.35090496733375371850 | q57 = 0.86342625760635763892 |
| q66 = 0 | q67 = 0 |
| q76 = -0.78956252086787838706 | q77 = 0 |
| q08 = 0 | q09 = 0 |
| q18 = 0 | q19 = 0 |
| q28 = 0 | q29 = 0 |
| q38 = 0.00075557026107702591326 | q39 = 0 |
| q48 = 0.0033052965252138828252 | q49 = -0.035124618972764619908 |
| q58 = 0.0010627906734254224064 | q59 = -0.011294029799477757896 |
| q68 = 0.0014730159164782497904 | q69 = -0.015653398238988014629 |
| q78 = 0.0013470034644502469271 | q79 = -0.014314293160353361934 |
| q010 = 0 | q011 = 0 |
| q110 = 0 | q111 = 0 |
| q210 = 0 | q211 = 0 |
| q310 = 0 | q311 = 0 |
| q410 = 0 | q411 = 0 |
| q510 = 0.058473528577946443849 | q511 = 0 |
| q610 = 0.081043652754640918266 | q611 = -0.28738393479202890305 |
| q710 = 0.074110591617504789877 | q711 = -0.26279903119968949743 |
| q012 = 0 | |
| q112 = 0 | |
| q212 = 0 | |
| q312 = 0 | |
| q412 = 0 | |
| q512 = 0 | |
| q612 = 0 | |
| q712 = 0.84914560513122095062 | |

6.2 Modified SBP-4-8(10) operator with diagonal norm and smaller spectral radius

| | |
|-----------------------------|----------------------------|
| q00 = -1.695766991157320 | q01 = 2.291032605468909 |
| q10 = -0.4426726432456110 | q11 = 0 |
| q20 = 0.5330534182148309 | q21 = -2.407040818496168 |
| q30 = -0.1184427737693269 | q31 = 0.6618843657314521 |
| q40 = 1.830612773966382 | q41 = -8.288032061663463 |
| q50 = -0.6245601110692797 | q51 = 2.709330688538044 |
| q60 = 0.3850559271659521 | q61 = -1.714360699440487 |
| q70 = -0.05705219972778544 | q71 = 0.2742239481189889 |
| q02 = -0.4639662012147939 | q03 = 0.7228532812132124 |
| q12 = 0.4048092994116597 | q13 = -0.7805039834619138 |
| q22 = 0 | q23 = 11.03207597325678 |
| q32 = -1.573371461527950 | q33 = 0 |
| q42 = 14.02365705116605 | q43 = -10.10065328335495 |
| q52 = -4.343572255913729 | q53 = 3.002892932574174 |
| q62 = 2.860630607831792 | q63 = -2.082622244166414 |
| q72 = -0.4973385909142549 | q73 = 0.3800614179644372 |
| q04 = -2.553891864910215 | q05 = 2.70983565186940 |
| q14 = 2.234132119994110 | q15 = -2.27133994516961 |
| q24 = -22.47769049395616 | q25 = 21.6521061372589 |
| q34 = 2.308946619504642 | q35 = -2.13484805031142 |
| q44 = 0 | q45 = 3.77017058952430 |
| q54 = -1.212267071714534 | q55 = 0 |
| q64 = 0.6108231151820283 | q65 = -0.690362730945967 |
| q74 = -0.06793041339961766 | q75 = 0.0990714324530388 |
| q06 = -1.20540452249925 | q07 = 0.1953080412300543 |
| q16 = 1.03696146986553 | q17 = -0.1813863173941616 |
| q26 = -10.2885737022032 | q27 = 1.956069485925045 |
| q36 = 1.06826234200632 | q37 = -0.2131866118947915 |
| q46 = -1.37062437516525 | q47 = 0.1666886279744916 |
| q56 = 0.498101251671513 | q57 = -0.07816772353808257 |
| q66 = 0 | q67 = 0.8513566887329923 |
| q76 = -0.778525470347940 | q77 = 0 |
| q08 = 0 | q09 = 0 |
| q18 = 0 | q19 = 0 |
| q28 = 0 | q29 = 0 |
| q38 = 0.0007555702610770257 | q39 = 0 |
| q48 = -0.03512461897276456 | q49 = 0.003305296525213877 |
| q58 = 0.05847352857794642 | q59 = -0.01129402979947775 |
| q68 = -0.2873839347920289 | q69 = 0.08104365275464091 |
| q78 = 0.8491456051312209 | q79 = -0.2627990311996895 |

| | |
|------------------------------|-------------------------------|
| q010 = 0 | q011 = 0 |
| q110 = 0 | q111 = 0 |
| q210 = 0 | q211 = 0 |
| q310 = 0 | q311 = 0 |
| q410 = 0 | q411 = 0 |
| q510 = 0.001062790673425422 | q511 = 0 |
| q610 = -0.01565339823898801 | q611 = 0.00147301591647824960 |
| q710 = 0.0741105916175047861 | q711 = -0.0143142931603533612 |
| q012 = 0 | |
| q112 = 0 | |
| q212 = 0 | |
| q312 = 0 | |
| q412 = 0 | |
| q512 = 0 | |
| q612 = 0 | |
| q712 = 0.001347003464450247 | |

REFERENCES

1. M.H. Carpenter, D. Gottlieb, and S. Abarbanel. Time-Stable Boundary Conditions for Finite-Difference Schemes Solving Hyperbolic Systems: Methodology and Application to High-Order Compact Schemes. *J. Comp. Phys.*, 111:220–236, (1994).
2. B. Gustafsson, H.-O. Kreiss, and J. Oliger. *Time Dependent Problems and Difference Methods*. John Wiley & Sons, New York, (1995).
3. H.-O. Kreiss and G. Scherer. Finite Element and Finite Difference Methods for Hyperbolic Partial Differential Equations. In C. De Boor, editor, *Mathematical Aspects of Finite Elements in Partial Differential Equations.*, pages 195–211. Academic Press, Inc., (1974).
4. B. Strand. Summation by Parts for Finite Difference Approximations for d/dx . *J. Comp. Phys.*, 110:47–67, (1994).
5. C.K.W Tam and Webb J. C. Dispersion-Relation-Preserving Finite Difference Schemes for Computational Acoustics. *J. Comp. Phys.*, 107:262–281, (1993).

Paper C

HIGH ORDER SUMMATION BY PARTS OPERATOR BASED ON A DRP SCHEME APPLIED TO 2D AEROACOUSTICS

Stefan Johansson

Division of Scientific Computing
Department of Information Technology
Uppsala University
P.O. Box 337
SE 75105 Uppsala
Sweden

Abstract

A strictly stable high order finite difference method based on Tam and Webb's dispersion relation preserving scheme in the interior has been verified for a 2D aeroacoustic problem. Results show that the method gives lower dispersion error than a similar method derived by Strand [11], which is based on standard sixth order difference approximation in the interior, when boundary effects are not important.

1 Introduction

Numerical simulation of wave propagation problems has been studied using computers for the last 50 years and is still actively studied. For the last 10 years computational aeroacoustics (CAA) has emerged as a sub-field. In CAA sound generation and sound propagation are modeled by the Navier-Stokes or Euler equations. High accuracy is required due to long time integration, leading to the need of highly accurate numerical methods.

Tam and Webb introduced Dispersion Preserving Relation (DRP) schemes [13] that give a better approximation of the wave number than standard finite difference schemes, thus giving a smaller dispersion error.

One of the more difficult problems for finite difference approximation is how to apply numerical boundary conditions in a stable way. One approach proposed by Kreiss and Scherer called summation by parts (SBP) [7] is to devise methods that give the same energy estimate as for the continuous problem. Thus, the SBP methods are strictly stable by construction and one does not have to use the algebraically difficult GKS theory [5] to prove stability.

High accuracy and strict stability have been combined in [6], where theoretical results and experimental verification were presented for a model problem in 1D. The main contribution of the present paper is the application of the resulting method to aeroacoustic wave propagation in 2D

[12]. The propagation of acoustic, entropy and vorticity waves is computed using the linearized 2D Euler equations. In addition we discuss the application of numerical dissipation where the damping does not affect the better resolution of the DRP method compared to a standard finite difference method.

The outline of the paper is as follows. In Section 2, we introduce the 2D linearized Euler equations to model sound propagation. In Section 3, the theory for a scalar test case in 1D is recapitulated, using the energy method to give an energy estimate for the continuous problem and explaining summation by parts which gives the same estimate in a discrete norm, cf. [4]. A discussion on how to apply artificial dissipation to Dispersion Relation Preserving schemes is given as well. In Section 4 numerical results that verify the numerical method are presented for a problem in computational aeroacoustics.

2 2D Linearized Euler Equations

The linearized Euler equations in conservative form [1] are used as a model of sound propagation. Denoting density ρ , velocity in x -direction u , in y -direction v , specific total energy E , specific total enthalpy H and pressure p . The equations are formulated in the variables ρ' , $(\rho u)'$, $(\rho v)'$ and $(\rho E)'$ that are perturbations of a reference state ρ_0 , $\rho_0 u_0$, $\rho_0 v_0$, $\rho_0 E_0$.

$$\begin{aligned} \frac{\partial}{\partial t} \begin{pmatrix} \rho' \\ (\rho u)' \\ (\rho v)' \\ (\rho E)' \end{pmatrix} + \frac{\partial}{\partial x} \begin{pmatrix} (\rho u)' \\ \rho_0 u_0 u' + (\rho u)' u_0 + p' \\ \rho_0 v_0 u' + (\rho v)' u_0 \\ \rho_0 H_0 u' + (\rho H)' u_0 \end{pmatrix} + \\ \frac{\partial}{\partial y} \begin{pmatrix} (\rho v)' \\ \rho_0 u_0 v' + (\rho u)' v_0 \\ \rho_0 v_0 v' + (\rho v)' v_0 + p' \\ \rho_0 H_0 v' + (\rho H)' v_0 \end{pmatrix} = 0 \quad (1) \end{aligned}$$

The acoustic quantities are defined by $\rho' = \rho - \rho_0$, $(\rho u)' = \rho u - \rho_0 u_0$, $(\rho v)' = \rho v - \rho_0 v_0$ and $(\rho E)' = \rho E - \rho_0 E_0$. With $(\rho H)' = (\rho E)' + p'$.

The variables u' , v' and p' can be calculated using

$$\mathbf{u}' = \frac{(\rho \mathbf{u})' - \rho' \mathbf{u}_0}{\rho_0} \quad (2)$$

$$p' = (\gamma - 1) \left((\rho E)' - \frac{1}{2} (2 (\rho \mathbf{u})' \cdot \mathbf{u}_0 - \rho' \mathbf{u}_0 \cdot \mathbf{u}_0) \right) \quad (3)$$

with $\mathbf{u} = (u, v)^T$

3 Theory

To make the paper self-contained the theory for a scalar test problem in 1D is recapitulated below.

3.1 Energy Method

A sufficient condition for well-posedness for an initial boundary value problem is to give a bound on the solution in terms of the initial value and boundary data, an energy estimate.

For example, introduce the L_2 scalar product and norm

$$(u, v) = \int_0^1 uv dx, \quad \|u\|^2 = (u, u). \quad (4)$$

We have for the simplest hyperbolic equation, sometimes called the Kreiss equation

$$\begin{cases} u_t &= u_x, \quad x \in [0, 1], t \geq 0 \\ u(x, 0) &= f(x), \quad x \in [0, 1] \\ u(1, t) &= g(t) \quad t \geq 0 \end{cases} \quad (5)$$

the following energy estimate

$$\frac{d\|u\|^2}{dt} = (u, u_t) + (u_t, u) = (u_x, u) + (u, u_x) = [u^2]_0^1 = g^2(t) - u^2(0, t). \quad (6)$$

That leads to an estimate on the norm of u in terms of the initial and boundary data [4].

3.2 Summation by parts

In the semi-discrete case we want to find an operator Q approximating d/dx and a discrete norm, $\|u\|^2 = (u, u)_H = u^T H u$, such that the semi-discretization of (5) gives the same estimate as the continuous case, where u and v are grid functions on $[0, 1]$ with step size h and H is a diagonal positive definite matrix. The energy method on $u_t = Qu$ gives

$$\frac{d\|u\|_H^2}{dt} = (u, u_t)_H + (u_t, u)_H = (u, Qu)_H + (Qu, u)_H = u^T (HQ + (HQ)^T) u \quad (7)$$

The same estimate as in the continuous is given if $(u, Qu)_H + (Qu, u)_H = [u^2]_0^1$, or equivalent $HQ + (HQ)^T = \text{diag}(-1, 0, \dots, 0, 1)$. This property is called summation by parts (SBP).

Operators with this property were proposed by Kreiss and Scherer [7] and extended to high order by Strand [11]. In [6] SBP operators for difference schemes of Dispersion Relation Preserving (DRP) schemes described in Section 3.3 type were developed.

3.3 Dispersion Relation Preserving Schemes

If the formal accuracy of a finite difference method is lowered by two orders as proposed by Tam and Webb [13] a free parameter is given that can be chosen such that the wave number is approximated better.

That free parameter ϕ is chosen such that error $E(\phi)$ in the approximation of the wave number is minimized

$$E(\phi) = \int_{-\pi/2}^{\pi/2} |hk - h\tilde{k}(\phi)|^2 d(hk) \quad (8)$$

where k and \tilde{k} are the exact and the approximate wave numbers, respectively.

A comparison between standard centered finite difference methods and the DRP schemes is given in Figure (1). The straight line shows the exact non-dimensional wave number hk . The dotted, dotted-dashed and dashed lines show the approximate non-dimensional wave numbers \tilde{hk} for different schemes. As seen the fourth order DRP scheme derived from the sixth order standard centered difference method gives a good approximation for the non-dimensional wave numbers up to about $\pi/2$ whereas the standard sixth order method gives a good approximation up to about 1.2. The details of the present fourth order DRP scheme and 6th, 8th order DRP schemes can be found in [6].

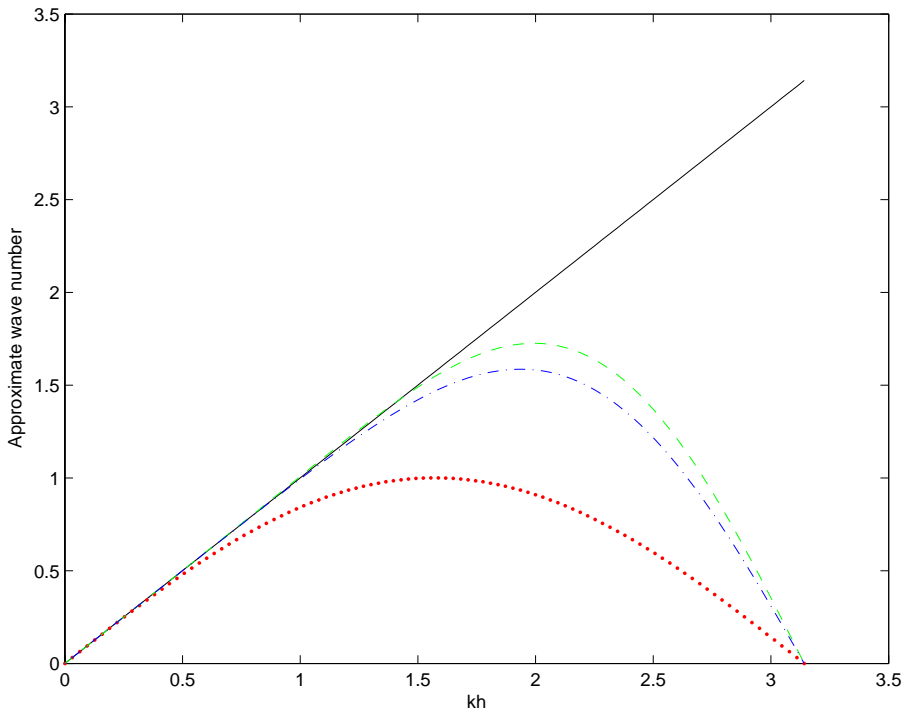


Figure 1: Approximate non-dimensional wave number vs exact for 2nd order standard centered difference method (SC2) (dotted), SC6 (dot-dashed), 4th order DRP scheme (dashed).

3.4 Numerical Dissipation

To damp high frequency modes in the numerical solution that are under-resolved artificial dissipation is often applied. The standard explicit type is $(-1)^{p+1} \beta (h^2 D_+ D_-)^p$, where $\beta > 0$ and $p \geq 1$.

But since DRP schemes are derived so that they give a good approximation for wave numbers less than $\pi/2$, very high order dissipation has to be used not to destroy that property. Figure 2 shows the Fourier transform of low pass filters for $p = 1 \dots 4$ which demonstrate that the damping is significant for wave numbers $< \pi/2$. Alternatives are to optimize the stencil in the artificial dissipation analogously to to use the idea proposed for filters by [2] or using an implicit artificial dissipation similar to the

idea used for filters proposed by [14].

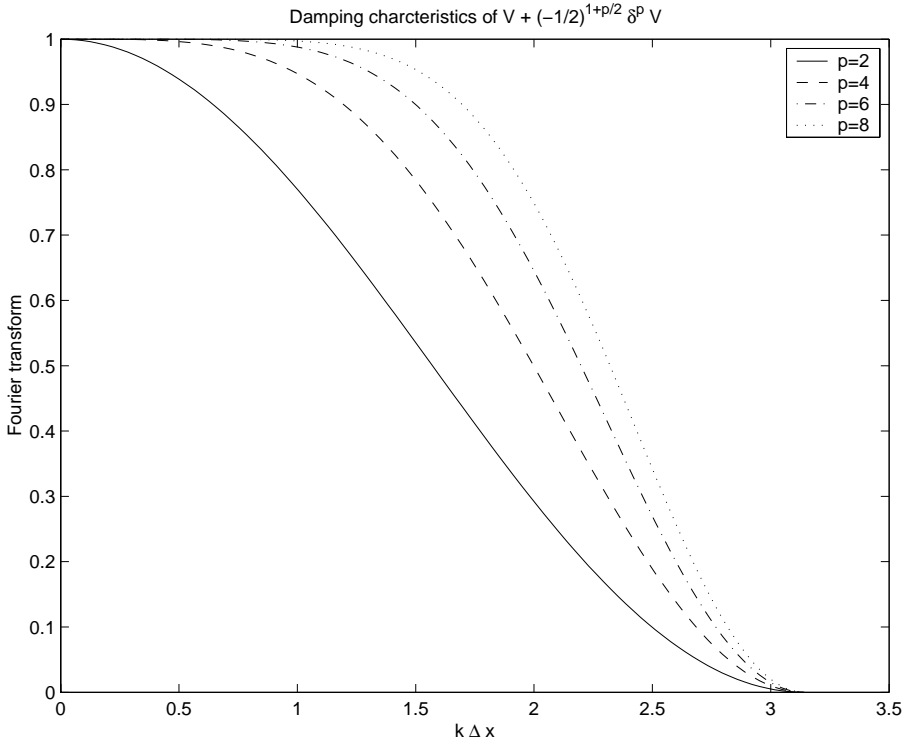


Figure 2: Fourier transform of low pass filters of orders 2, 4, 6, 8.

Assume that S is a dissipation operator, the energy method on the Kreiss equation in semi discrete form with dissipation added $u_t = Qu + H^{-1}Su$ gives

$$\frac{d}{dt} \|u\|_H = (u_t, u)_H + (u, u_t)_H = (Qu + Su, u)_H + (u, Qu + Su)_H = u^T (HQ + (HQ)^T + S + S^T)u \quad (9)$$

If the interior stencil of S is $(-1)^{p+1}\beta(h^2 D_+ D_-)^p$ a boundary closure that guarantees that $S + S^T \leq 0$ can be found [3] [8].

Using an implicit dissipation $(-1)^{p+1}\beta P^{-1}(h^2 D_+ D_-)^p$, where P is a symmetric tridiagonal matrix with ones on the diagonal does not give an energy estimate with the standard boundary closure for $p = 1, 2, 3$, which was verified numerically. In general nothing can be said about the definiteness of $P^{-1}S$.

4 Application to a 2D aeroacoustic problem

The high order SBP operator based on the Tam and Webb DRP scheme was implemented in a FORTRAN program [10] and tested for an aero-

coustic test problem. The results were compared with those obtained with a SBP operator based on a standard central finite difference stencil.

The 2D linearized Euler equations described in Section 2 were solved using those SBP operators to discretize x and y derivatives and using the standard fourth order Runge-Kutta method to discretize the time derivative.

A benchmark problem was chosen from [12], choosing $u_0 = 0.5$, $v_0 = 0$ with the following initial condition

$$p'(x, y, 0) = e^{-\log(2)\frac{x^2+y^2}{9}} \quad (10)$$

$$\rho'(x, y, 0) = e^{-\log(2)\frac{x^2+y^2}{9}} + 0.1e^{-\log(2)\frac{(x-67)^2+y^2}{25}} \quad (11)$$

$$u'(x, y, 0) = 0.04ye^{-\log(2)\frac{(x-67)^2+y^2}{25}} \quad (12)$$

$$v'(x, y, 0) = -0.04(x-67)e^{-\log(2)\frac{(x-67)^2+y^2}{25}} \quad (13)$$

to the linearized Euler equations. There exists an analytical solution for verification of the numerical results [12].

Numerical solution obtained with the DRPSBP scheme for ρ' , the acoustic density, with the two resolutions at time instant $T = 40$ can be found in Figure 3, near the center the acoustic pulse is seen, propagating with the speed of sound in all directions transported with the mean velocity. Near the right boundary the entropy and vorticity wave is seen propagating with the mean velocity.

The time instances were deliberately chosen such that the solution had not reached the boundary, since the non reflecting boundary condition implemented is not of high order and the purpose of this paper is to evaluate the new SBP method. Results for the first order Enquist-Majda boundary condition can be found in [10]

Figure 4 to Figure 7 show the numerical solution using SBP-3-6 (SBP operator based on the sixth order standard finite difference scheme with third order near the boundaries) compared to DRPSBP-2-4 (SBP operator based on a fourth order DRP scheme derived from a sixth order standard finite difference scheme with second order near the boundaries) of ρ' along the x -axis at time $T = 40$, compared to the exact solution for two different grid sizes, and with and without filtering. The filter is applied in each time step and of standard type $(-1)^{p+1}2^{-2p}(h^2D_+D_-)^p$, in this case $p = 3$ is chosen [9], with the boundary treatment according to [3].

Figure 4 shows that the method based on a DRP scheme has lower dispersion error and has more accurate peak values, and smaller amplitudes on the wiggles but more noticeable overshoots. The entropy and vorticity wave at $x = 87$ is better resolved than the acoustic waves at $x = -20$ and $x = 60$. Table 1 and Table 5 show that DRPSBP-2-4 has about a 60 % lower L_2 -error along the x -axis for the lower resolution.

When refining the grid the differences between the methods are not seen in Figure 5. Table 2 and Table 6 show that the difference in L_2 -error along the x -axis is about 10 %, but to advantage of the SBP method.

On the other hand when applying a standard type filter to damp the high frequency oscillations, there is less difference between the methods as shown in Figure 6 and Figure 7. Table 3, Table 4, Table 7 and Table 8 stating the L_2 -error along the x -axis for the two grid sizes and the two time instances chosen, demonstrate that the L_2 -error along the x -axis is larger than without filtering. The reason is that the filter imposes

significant damping for wave numbers $hk < \pi/2$ cf. Figure 2, which affects the higher resolution of the DRP based SBP method.

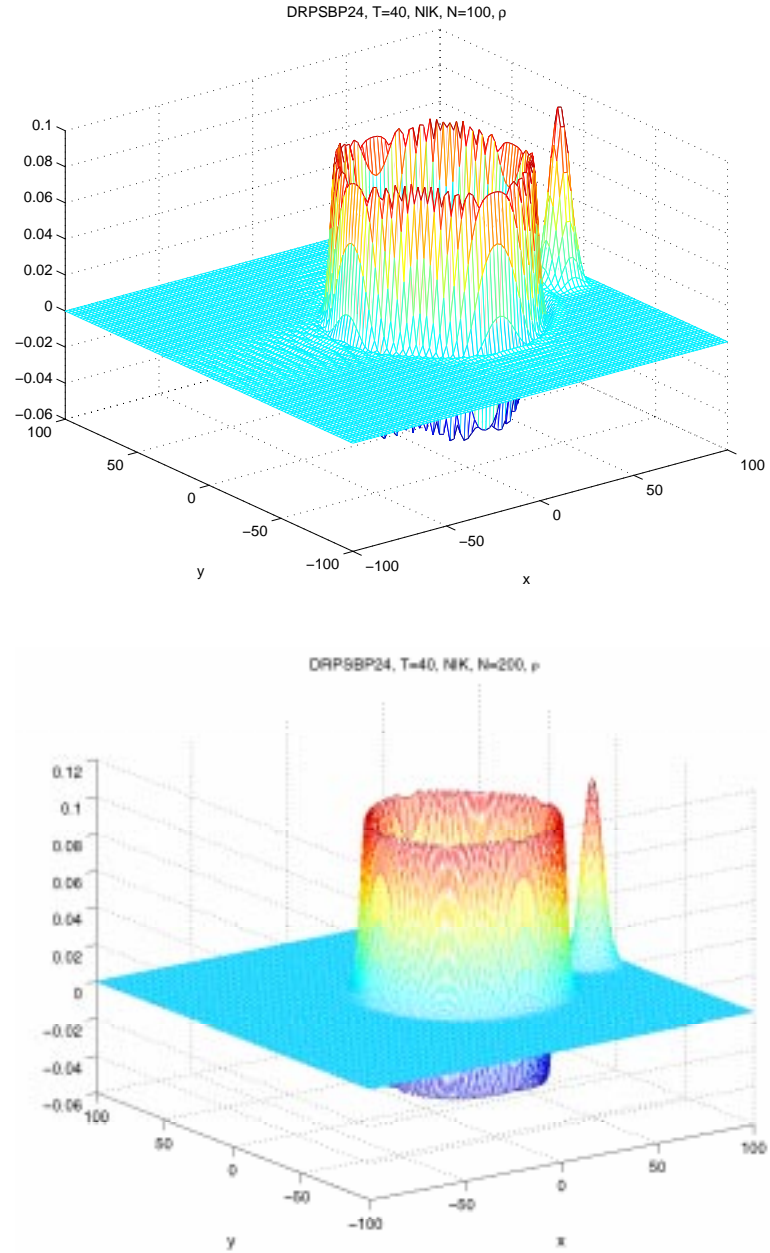


Figure 3: Surface plot of acoustic density at time 40, without filtering, top: N=101, bottom: N=201.

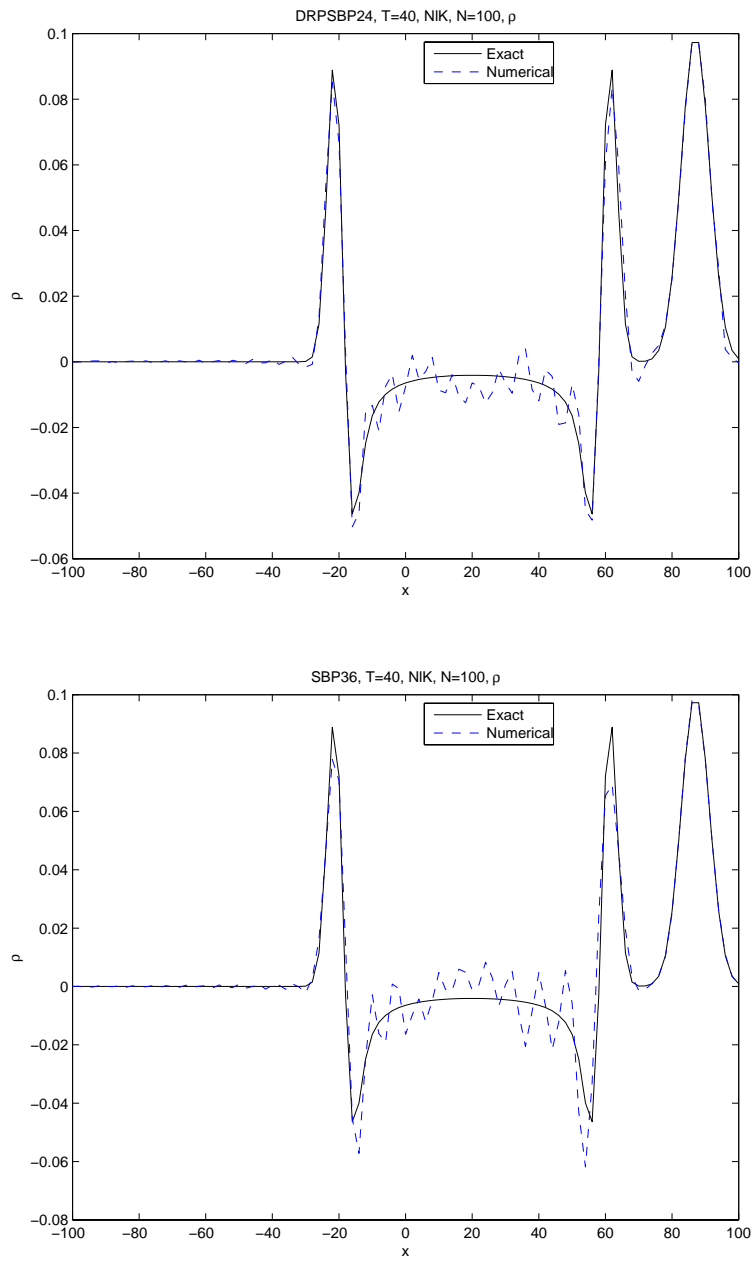


Figure 4: Numerical solution of ρ' at time 40, $N = 101$, without filtering, top: DRPSBP-2-4, bottom: SBP-3-6.

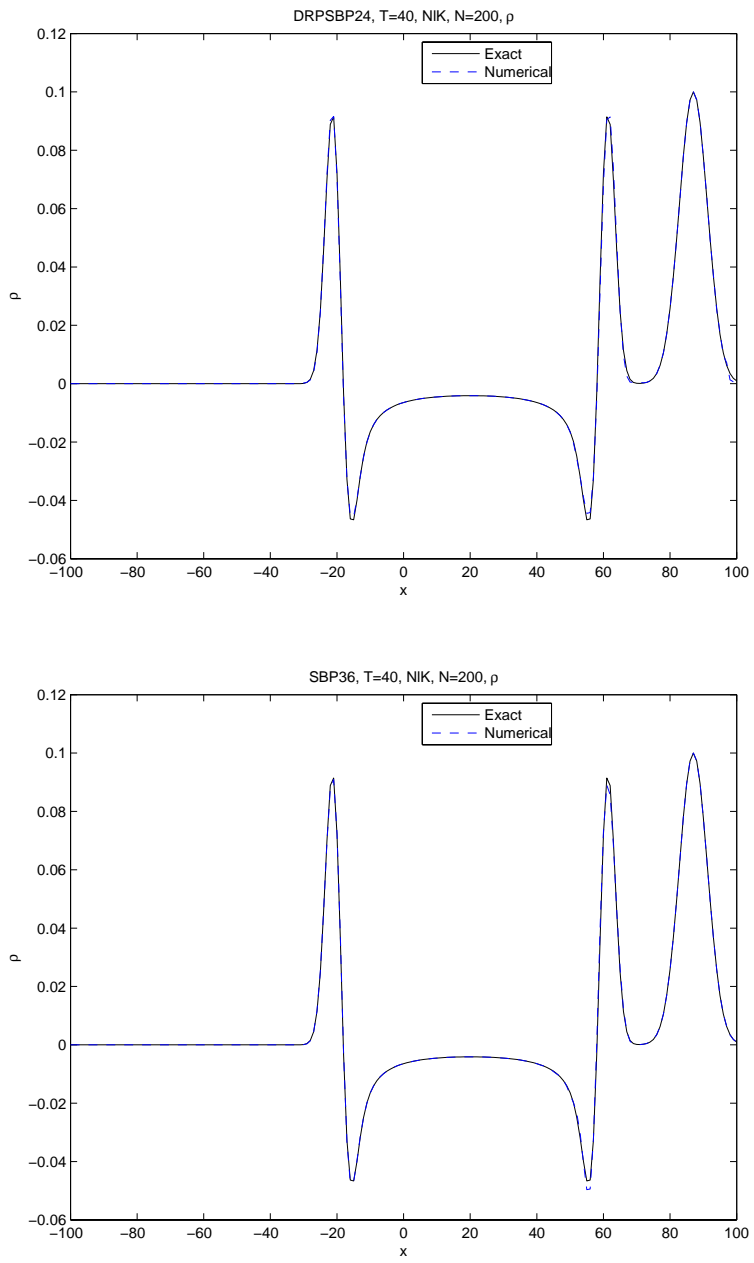


Figure 5: Numerical solution of ρ' at time 40, $N = 201$, without filtering, top: DRPSBP-2-4, bottom: SBP-3-6.

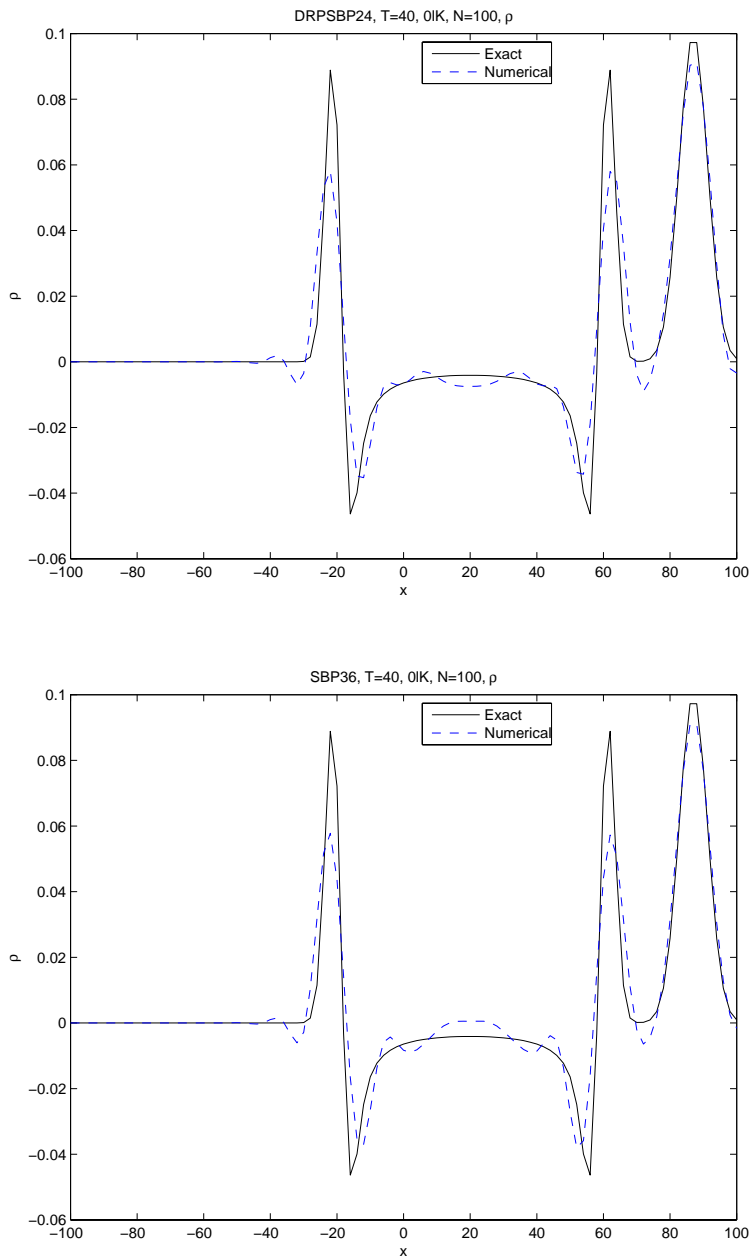


Figure 6: Numerical solution of ρ' at time 40, $N = 101$, sixth order filter, top: DRPSBP-2-4, bottom: SBP-3-6.

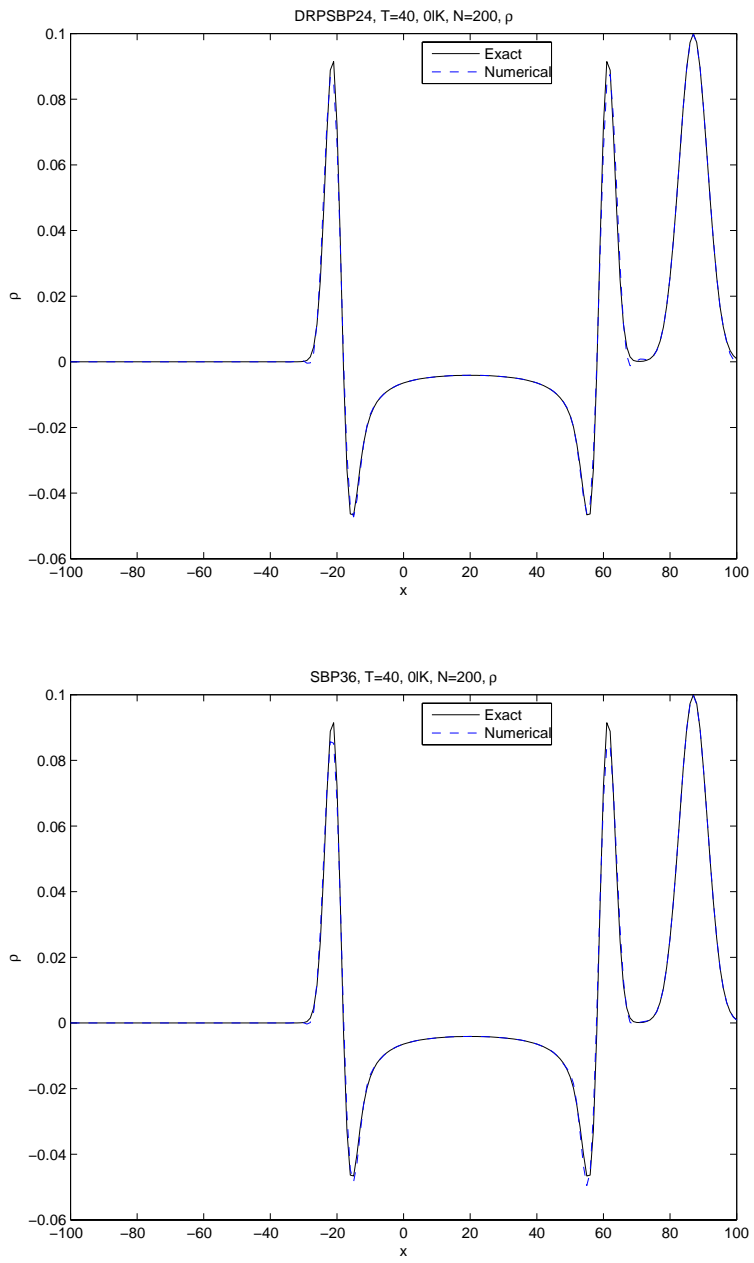


Figure 7: Numerical solution of ρ' at time 40, $N = 201$, sixth order filter, top: DRPSBP-2-4, bottom: SBP-3-6.

| | DRPSBP-2-4 | SBP-3-6 |
|--|------------|------------|
| L2-error along the x -axis in ρ | 0.00431254 | 0.00788948 |
| L2-error along the x -axis in p | 0.00431147 | 0.00788902 |
| L2-error along the x -axis in u | 0.00428112 | 0.00649726 |

Table 1: $u_0=0.5$, $T=20$, $N = 101$, no filter

| | DRPSBP-2-4 | SBP-3-6 |
|--|------------|------------|
| L2-error along the x -axis in ρ | 0.00049776 | 0.00047037 |
| L2-error along the x -axis in p | 0.00049762 | 0.00047037 |
| L2-error along the x -axis in u | 0.00049358 | 0.00046720 |

Table 2: $u_0=0.5$, $T=20$, $N = 201$, no filter

| | DRPSBP-2-4 | SBP-3-6 |
|--|------------|------------|
| L2-error along the x -axis in ρ | 0.01022241 | 0.01020396 |
| L2-error along the x -axis in p | 0.01018905 | 0.01017082 |
| L2-error along the x -axis in u | 0.00991698 | 0.00986553 |

Table 3: $u_0=0.5$, $T=20$, $N = 101$, sixth order filter

| | DRPSBP-2-4 | SBP-3-6 |
|--|------------|------------|
| L2-error along the x -axis in ρ | 0.00118599 | 0.00114419 |
| L2-error along the x -axis in p | 0.00118562 | 0.00114392 |
| L2-error along the x -axis in u | 0.00117612 | 0.00113471 |

Table 4: $u_0=0.5$, $T=20$, $N = 201$, sixth order filter

| | DRPSBP-2-4 | SBP-3-6 |
|--|------------|------------|
| L2-error along the x -axis in ρ | 0.00444214 | 0.00723430 |
| L2-error along the x -axis in p | 0.00436382 | 0.00723236 |
| L2-error along the x -axis in u | 0.00372037 | 0.00676451 |

Table 5: $M=0.5$, $T=40$, $N = 101$, no filter

| | DRPSBP-2-4 | SBP-3-6 |
|--|------------|------------|
| L2-error along the x -axis in ρ | 0.00074894 | 0.00063326 |
| L2-error along the x -axis in p | 0.00071616 | 0.00063313 |
| L2-error along the x -axis in u | 0.00071466 | 0.00063204 |

Table 6: $u_0=0.5$, $T=40$, $N = 201$, no filter

| | DRPSBP-2-4 | SBP-3-6 |
|--|------------|------------|
| L2-error along the x -axis in ρ | 0.00903172 | 0.00910053 |
| L2-error along the x -axis in p | 0.00885448 | 0.00895898 |
| L2-error along the x -axis in u | 0.00879172 | 0.00881355 |

Table 7: $u_0=0.5$, $T=40$, $N = 101$, sixth order filter

| | DRPSBP-2-4 | SBP-3-6 |
|--|------------|------------|
| L2-error along the x -axis in ρ | 0.00148481 | 0.00138574 |
| L2-error along the x -axis in p | 0.00147850 | 0.00138488 |
| L2-error along the x -axis in u | 0.00147532 | 0.00138194 |

Table 8: $u_0=0.5$, $T=40$, $N = 201$, sixth order filter

The numerical results for the 2D linearized Euler equations show that the better approximation of the wave number for the DRP based SBP operator of fourth order (second order near the boundary) results in a smaller L_2 -error than for a SBP operator based on standard sixth order (third order near the boundary) stencil. The results are valid when the problem is not fully resolved, which usually is the case for large scale applications.

Application of a sixth order filter affects the good wave approximation of the DRPSPB operator. That problem can be solved by using a filter or artificial dissipation that apply less dissipation for wave numbers $hk < \pi/2$ than the present filter.

5 Conclusions and Future Work

A strictly stable finite difference method with the summation by parts property (SBP) based on Tam and Webb's dispersion relation preserving (DRP) scheme in the interior developed in [6] has been tested on a 2D aeroacoustic problem. The results show that the SBP method based on the DRP scheme yields smaller errors for low resolutions without using a filter. But the advantage disappears with high resolution and/or using a sixth order explicit filter. However, using other types of artificial dissipation or filters, that are tailored to match the better wave number resolution of the DRP scheme, should lead to better results. Also in realistic applications it is often not possible to use the resolution needed, which shows the advantage of the DRPSBP method. The development and implementation of accurate non reflecting boundary conditions is future work. We also plan to develop high order numerical dissipation that will replace the filter used in this paper.

References

- [1] M. Billson, L.-E. Eriksson, and L. Davidson. Acoustic Source Terms for the Linear Euler Equations on Conservative Form. In *8th AIAA/CAES Aeroacoustics Conference*, Breckenridge, Colorado, (2002). AIAA Paper 2002-2582.
- [2] C. Bogey and C. Bailly. A family of low dispersive and low dissipative explicit schemes for flow and noise computations. *J. Comp. Phys.*, 194(1):194–214, (2004).
- [3] L.-E. Eriksson. Boundary conditions for artificial dissipation operators. Technical Report FFA TN 1984-53, The Aeronautical Research Institute of Sweden, (1984).
- [4] B. Gustafsson, H.-O. Kreiss, and J. Oliger. *Time Dependent Problems and Difference Methods*. John Wiley & Sons, New York, (1995).
- [5] B. Gustafsson, H.-O. Kreiss, and A. Sundström. Stability Theory of Difference Approximations for Mixed Initial Boundary Value Problems. II. *Math. Comp.*, 26(119):649–686, (1972).
- [6] S. Johansson. High Order Finite Difference Operators with the Summation by Parts Property Based on DRP Schemes. Technical Report 2004-035, Uppsala University, Department of Scientific Computing, 2004.
- [7] H.-O. Kreiss and G. Scherer. Finite Element and Finite Difference Methods for Hyperbolic Partial Differential Equations. In C. De Boor, editor, *Mathematical Aspects of Finite Elements in Partial Differential Equations.*, pages 195–211. Academic Press, Inc., (1974).
- [8] K. Mattsson, M. Svärd, and J. Nordström. Stable and Accurate Artificial Dissipation. *J. Sci. Comp.*, 21(1):57–79, (2004).
- [9] B. Müller and S. Johansson. Strictly Stable High Order Difference Approximations for Low Mach Number Aeroacoustics. In P. Neittaanmäki, T. Rossi, K. Majava, and O. Pironneau, editors, *ECCOMAS 2004*, 2004.
- [10] C. L. Müller. *High order accurate numerical solution of the linearized Euler equations for sound propagation in the atmosphere*. Master’s thesis, Uppsala University, Department of Scientific Computing, (2004).
- [11] B. Strand. Summation by Parts for Finite Difference Approximations for d/dx . *J. Comp. Phys.*, 110:47–67, (1994).
- [12] C.K.W. Tam. Benchmark Problems and Solutions. In J.C. Hardin, J.R. Ristorcelli, and C.K.W. Tam, editors, *ICASE/LaRC Workshop on Benchmark Problems in Computational Aeroacoustics (CAA)*, (1995). NASA CP 3300.
- [13] C.K.W Tam and J. C. Webb. Dispersion-Relation-Preserving Finite Difference Schemes for Computational Acoustics. *J. Comp. Phys.*, 107:262–281, (1993).
- [14] M. R. Visbal and D. V. Gaitonde. High-Order-Accurate Methods for Complex Unsteady Subsonic Flows. *AIAA J.*, 37(10):1231–1239, (1999).